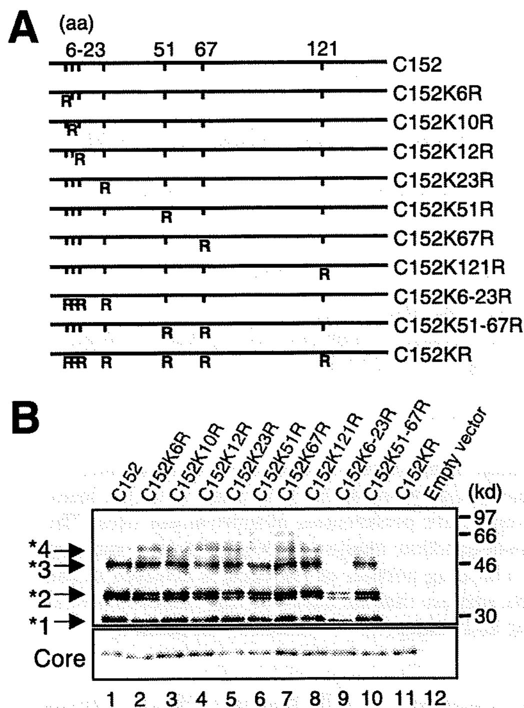

FIG. 1. In vivo ubiquitylation of HCV core protein. (A) The HCV core protein (N-terminal 152 aa) is represented on the top. The positions of the amino acid residues of the core protein are indicated above the bold lines. The positions of the seven Lys residues in the core are marked by vertical ticks. Substitution of Lys with Arg (R) is schematically depicted. (B) Detection of ubiquitylated forms of the core proteins. The transfected cells with core expression plasmids and pMT107 were treated with the proteasome inhibitor MG132 and harvested 48 h after transfection. His_6-tagged proteins were purified and subsequently analyzed by Western blot analysis using anticore antibody (upper panel). Core proteins conjugated to a number of His_6-Ub are denoted with asterisks. Whole lysates of transfected cells before purification were also analyzed (lower panel). Lanes 1 to 11, C152 to C152KR, as indicated for panel A. Lane 12; empty vector.

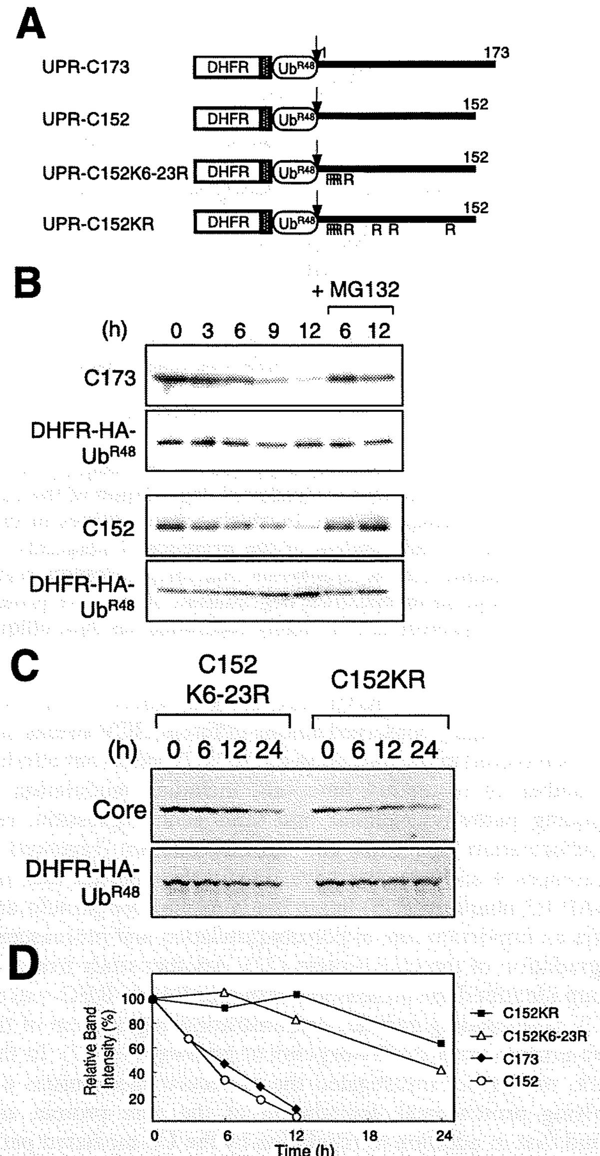

FIG. 2. Kinetic analysis of degradation of HCV core proteins. (A) The fusion constructs used in the UPR technique. Open boxes indicate the DHFR sequence, which is extended at the C terminus by a sequence containing the HA epitope (hatched boxes). Ub^{R48} moieties bearing the Lys-Arg substitution at aa 48 are represented by open ellipses. Bold lines indicate the regions of the core protein. The amino acid positions of the core protein are indicated above the bold lines. The arrows indicate the sites of in vivo cleavage by deubiquitylating enzymes. (B and C) Turnover of the core proteins. After a 24-h transfection with each UPR construct, cells were treated with 50 μg of cycloheximide/ml in the presence or absence of 10 μM MG132 for the different time periods indicated. Cells were lysed at the different time points indicated, followed by evaluation via sodium dodecyl sulfate-polyacrylamide gel electrophoresis and Western blot analysis using antibodies against the core protein and HA. (D) Quantitation of the data shown in panels B and C. At each time point, the ratio of band intensity of the core protein relative to the reference DHFR-HA-Ub^{R48} was determined by densitometry and is plotted as a percentage of the ratio at time zero.

tion with UPR constructs, cells were treated with cycloheximide and the amounts of core proteins and DHFR-HA-Ub^{R48} at the indicated time points were determined by Western blot analysis using anticore and anti-HA antibodies. The mature form of the core protein, aa 1 to 173 (C173) (13, 20), and C152 were degraded with first-order kinetics (Fig. 2B and D). MG132 completely blocked the degradation of C173 and C152 (Fig. 2B), and C152K6-23R and C152KR were markedly stabilized (Fig. 2C). The half-lives of C173 and C152 were calculated to be 5 to 6 h, whereas those of C152K6-23R and C152KR were calculated to be 22 to 24 h (Fig. 2D), confirming that the Ub plays an important role in regulating degradation of the core protein. Nevertheless, these results also suggest possible involvement of the Ub-independent pathway in the turnover of the core protein, as C152KR is more destabilized than the reference protein (Fig. 2C and 2D).

We have shown that PA28γ specifically binds to the core protein and is involved in its degradation (16, 17). Recent studies demonstrated that PA28γ is responsible for Ub-independent degradation of the steroid receptor coactivator SRC-3 and cell cycle inhibitors such as p21 (3, 11, 12). Thus, we next investigated the possibility of PA28γ involvement in the degradation of either C152KR or C152. Since C152KR carries two amino acid substitutions in the PA28γ-binding region (aa 44 to 71) (17), we tested the influence of the mutations of C152KR on the interaction with PA28γ by use of a coimmunoprecipi-

tation assay. When Flag-tagged PA28γ (F-PA28γ) was expressed in cells along with C152 or C152KR, F-PA28γ precipitated along with both C152 and C152KR, indicating that PA28γ interacts with both core proteins (Fig. 3A). Figure 3B reveals the effect of exogenous expression of F-PA28γ on the steady-state levels of C152 and C152KR. Consistent with previous data (17), the expression level of C152 was decreased to a nearly undetectable level in the presence of PA28γ (Fig. 3B, lanes 1 and 3). Interestingly, exogenous expression of PA28γ led to a marked reduction in the amount of C152KR expressed (Fig. 3B, lanes 5 and 7). Treatment with MG132 increased the steady-state level of the C152KR in the presence of F-PA28γ as well as the level of C152 (Fig. 3B, lanes 4 and 8).

We further investigated whether PA28γ affects the turnover of Lys-less core protein through time course experiments. C152KR was rapidly destabilized and almost completely degraded in a 3-h chase experiment using cells overexpressing F-PA28γ (Fig. 3C, left panels). A similar result was obtained using an analogous Lys-less mutant of the full-length core protein C191KR (Fig. 3C, right panels), thus demonstrating that the Lys-less core protein undergoes proteasomal degradation in a PA28γ-dependent manner. These results suggest that PA28γ may play a role in accelerating the turnover of the HCV core protein that is independent of ubiquitylation.

Finally, we examined gain- and loss-of-function of PA28γ with respect to degradation of full-length wild-type (C191) and mutated (C191KR) core proteins in human hepatoma Huh-7 cells. As expected, exogenous expression of PA28γ or E6AP caused a decrease in the C191 steady-state levels (Fig. 4A). In contrast, the C191KR level was decreased with expression of PA28γ but not of E6AP. We further used RNA interference to inhibit expression of PA28γ or E6AP. An increase in the abundance of C191KR was observed with PA28γ small interfering RNA (siRNA) but not with E6AP siRNA (Fig. 4B). An increase in the C191 level caused by the activity of siRNA against PA28γ or E6AP was confirmed as well.

Taking these results together, we conclude that turnover of the core protein is regulated by both Ub-dependent and Ub-independent pathways and that PA28γ is possibly involved in Ub-independent proteasomal degradation of the core protein. PA28 is known to specifically bind and activate the 20S proteasome (19). Thus, PA28γ may function by facilitating the delivery of the core protein to the proteasome in a Ub-independent manner.

Accumulating evidence suggests the existence of proteasome-dependent but Ub-independent pathways for protein degradation, and several important molecules, such as p53, p73, Rb, SRC-3, and the hepatitis B virus X protein, have two distinct degradation pathways that function in a Ub-dependent and Ub-independent manner (1, 2, 6, 7, 14, 21, 27). Recently, critical roles for PA28γ in the Ub-independent pathway have been demonstrated; SRC-3 and p21 can be recognized by the 20S proteasome independently of ubiquitylation through their interaction with PA28γ (3, 11, 12). It has also been reported that phosphorylation-dependent ubiquitylation mediated by GSK3 and SCF is important for SRC-3 turnover (26). Nevertheless, the precise mechanisms underlying turnover of most of the proteasome substrates that are regulated in both Ub-dependent and Ub-independent manners are not well understood. To our knowledge, the HCV core protein is the first

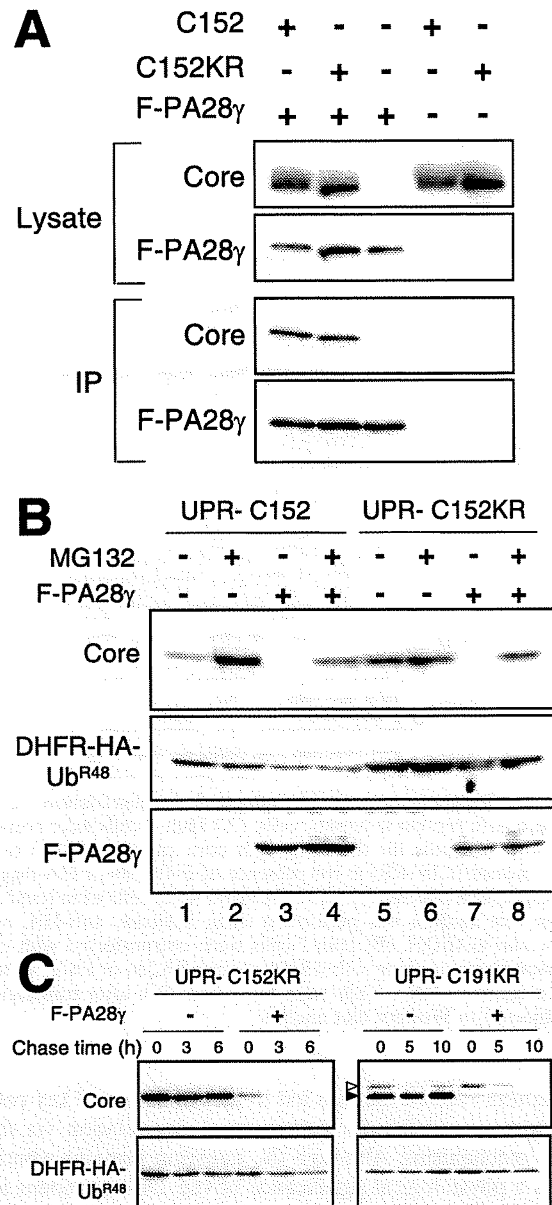

FIG. 3. PA28γ-dependent degradation of the core protein. (A) Interaction of the core protein with PA28γ. Cells were cotransfected with the wild-type (C152) or Lys-less (C152KR) core expression plasmid in the presence of a Flag-PA28γ (F-PA28γ) expression plasmid or an empty vector. The transfected cells were treated with MG132. After 48 h, the cell lysates were immunoprecipitated with anti-Flag antibody and visualized by Western blotting with anticore antibodies. Western blot analysis of whole cell lysates was also performed. (B) Degradation of the wild-type and Lys-less core proteins via the PA28γ-dependent pathway. Cells were transfected with the UPR construct with or without F-PA28γ. In some cases, cells were treated with 10 μM MG132 for 14 h before harvesting. Western blot analysis was performed using anticore, anti-HA, and anti-Flag antibodies. (C) After 24 h of transfection with UPR-C152KR and UPR-C191KR with or without F-PA28γ (an empty vector), cells were treated with 50 μg of cycloheximide/ml for different time periods as indicated (chase time). Western blot analysis was performed using anticore and anti-HA antibodies. The precursor core protein and the core that was processed, presumably by signal peptide peptidase, are denoted by open and closed triangles, respectively.

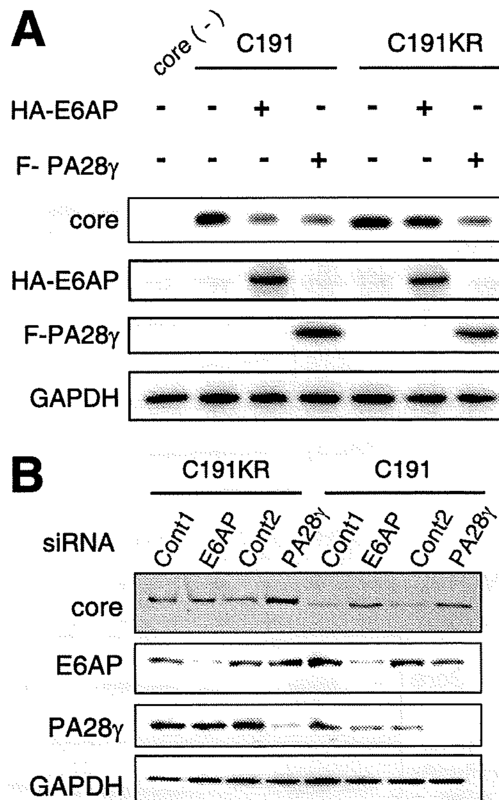

FIG. 4. Ub-dependent and Ub-independent degradation of the full-length core protein in hepatic cells. (A) Huh-7 cells were cotransfected with plasmids for the full-length core protein (C191) or its Lys-less mutant (C191KR) in the presence of F-PA28γ or HA-tagged-E6AP expression plasmid (HA-E6AP). After 48 h, cells were lysed and Western blot analysis was performed using anticore, anti-HA, anti-Flag, or anti-GAPDH. (B) Huh-7 cells were cotransfected with core expression plasmids along with siRNA against PA28γ or E6AP or with negative control siRNA. Cells were harvested 72 h after transfection and subjected to Western blot analysis.

viral protein studied that has led to identification of key cellular factors responsible for proteasomal degradation via dual distinct mechanisms. Although the question remains whether there is a physiological significance of the Ub-dependent and Ub-independent degradation of the core protein, it is reasonable to consider that tight control over cellular levels of the core protein, which is multifunctional and essential for viral replication, maturation, and pathogenesis, may play an important role in representing the potential for its functional activity.

This work was supported by a grant-in-aid for Scientific Research from the Japan Society for the Promotion of Science, from the Ministry of Health, Labor and Welfare of Japan, and from the Ministry of Education, Culture, Sports, Science and Technology, by Research on Health Sciences focusing on Drug Innovation from the Japan Health Sciences Foundation, Japan, and by the Program for Promotion of Fundamental Studies in Health Sciences of the National Institute of Biomedical Innovation of Japan.

REFERENCES

1. **Asher, G., J. Lotem, L. Sachs, C. Kahana, and Y. Shaul.** 2002. Mdm-2 and ubiquitin-independent p53 proteasomal degradation regulated by NQO1. Proc. Natl. Acad. Sci. USA **99:**13125–13130.
2. **Asher, G., P. Tsvetkov, C. Kahana, and Y. Shaul.** 2005. A mechanism of ubiquitin-independent proteasomal degradation of the tumor suppressors p53 and p73. Genes Dev. **19:**316–321.
3. **Chen, X., L. F. Barton, Y. Chi, B. E. Clurman, and J. M. Roberts.** 2007. Ubiquitin-independent degradation of cell-cycle inhibitors by the REGγ proteasome. Mol. Cell **26:**843–852.
4. **Ciechanover, A.** 1998. The ubiquitin-proteasome pathway: on protein death and cell life. EMBO J. **17:**7151–7160.
5. **Hershko, A., A. Ciechanover, and A. Varshavsky.** 2000. The ubiquitin system. Nat. Med. **6:**1073–1081.
6. **Jariel-Encontre, I., M. Pariat, F. Martin, S. Carillo, C. Salvat, and M. Piechaczyk.** 1995. Ubiquitinylation is not an absolute requirement for degradation of c-Jun protein by the 26 S proteasome. J. Biol. Chem. **270:**11623–11627.
7. **Jin, Y., H. Lee, S. X. Zeng, M. S. Dai, and H. Lu.** 2003. MDM2 promotes p21waf1/cip1 proteasomal turnover independently of ubiquitylation. EMBO J. **22:**6365–6377.
8. **Ju, D., and Y. Xie.** 2006. Identification of the preferential ubiquitination site and ubiquitin-dependent degradation signal of Rpn4. J. Biol. Chem. **281:**10657–10662.
9. **Lai, M. M. C., and C. F. Ware.** 1999. Hepatitis C virus core protein: possible roles in viral pathogenesis. Springer, Berlin, Germany.
10. **Lévy, F., N. Johnsson, T. Rumenapf, and A. Varshavsky.** 1996. Using ubiquitin to follow the metabolic fate of a protein. Proc. Natl. Acad. Sci. USA **93:**4907–4912.
11. **Li, X., L. Amazit, W. Long, D. M. Lonard, J. J. Monaco, and B. W. O'Malley.** 2007. Ubiquitin- and ATP-independent proteolytic turnover of p21 by the REGγ-proteasome pathway. Mol. Cell **26:**831–842.
12. **Li, X., D. M. Lonard, S. Y. Jung, A. Malovannaya, Q. Feng, J. Qin, S. Y. Tsai, M. J. Tsai, and B. W. O'Malley.** 2006. The SRC-3/AIB1 coactivator is degraded in a ubiquitin- and ATP-independent manner by the REGγ proteasome. Cell **124:**381–392.
13. **Liu, Q., C. Tackney, R. A. Bhat, A. M. Prince, and P. Zhang.** 1997. Regulated processing of hepatitis C virus core protein is linked to subcellular localization. J. Virol. **71:**657–662.
14. **Lonard, D. M., Z. Nawaz, C. L. Smith, and B. W. O'Malley.** 2000. The 26S proteasome is required for estrogen receptor-α and coactivator turnover and for efficient estrogen receptor-α transactivation. Mol. Cell **5:**939–948.
15. **Moradpour, D., F. Penin, and C. M. Rice.** 2007. Replication of hepatitis C virus. Nat. Rev. Microbiol. **5:**453–463.
16. **Moriishi, K., R. Mochizuki, K. Moriya, H. Miyamoto, Y. Mori, T. Abe, S. Murata, K. Tanaka, T. Miyamura, T. Suzuki, K. Koike, and Y. Matsuura.** 2007. Critical role of PA28γ in hepatitis C virus-associated steatogenesis and hepatocarcinogenesis. Proc. Natl. Acad. Sci. USA **104:**1661–1666.
17. **Moriishi, K., T. Okabayashi, K. Nakai, K. Moriya, K. Koike, S. Murata, T. Chiba, K. Tanaka, R. Suzuki, T. Suzuki, T. Miyamura, and Y. Matsuura.** 2003. Proteasome activator PA28γ-dependent nuclear retention and degradation of hepatitis C virus core protein. J. Virol. **77:**10237–10249.
18. **Niwa, H., K. Yamamura, and J. Miyazaki.** 1991. Efficient selection for high-expression transfectants with a novel eukaryotic vector. Gene **108:**193–199.
19. **Realini, C., C. C. Jensen, Z. Zhang, S. C. Johnston, J. R. Knowlton, C. P. Hill, and M. Rechsteiner.** 1997. Characterization of recombinant REGα, REGβ, and REGγ proteasome activators. J. Biol. Chem. **272:**25483–25492.
20. **Santolini, E., G. Migliaccio, and N. La Monica.** 1994. Biosynthesis and biochemical properties of the hepatitis C virus core protein. J. Virol. **68:**3631–3641.
21. **Sheaff, R. J., J. D. Singer, J. Swanger, M. Smitherman, J. M. Roberts, and B. E. Clurman.** 2000. Proteasomal turnover of p21Cip1 does not require p21Cip1 ubiquitination. Mol. Cell **5:**403–410.
22. **Shirakura, M., K. Murakami, T. Ichimura, R. Suzuki, T. Shimoji, K. Fukuda, K. Abe, S. Sato, M. Fukasawa, Y. Yamakawa, M. Nishijima, K. Moriishi, Y. Matsuura, T. Wakita, T. Suzuki, P. M. Howley, T. Miyamura, and I. Shoji.** 2007. E6AP ubiquitin ligase mediates ubiquitylation and degradation of hepatitis C virus core protein. J. Virol. **81:**1174–1185.
23. **Suzuki, R., K. Tamura, J. Li, K. Ishii, Y. Matsuura, T. Miyamura, and T. Suzuki.** 2001. Ubiquitin-mediated degradation of hepatitis C virus core protein is regulated by processing at its carboxyl terminus. Virology **280:**301–309.
24. **Suzuki, T., and A. Varshavsky.** 1999. Degradation signals in the lysine-asparagine sequence space. EMBO J. **18:**6017–6026.
25. **Treier, M., L. M. Staszewski, and D. Bohmann.** 1994. Ubiquitin-dependent c-Jun degradation in vivo is mediated by the δ domain. Cell **78:**787–798.
26. **Wu, R. C., Q. Feng, D. M. Lonard, and B. W. O'Malley.** 2007. SRC-3 coactivator functional lifetime is regulated by a phospho-dependent ubiquitin time clock. Cell **129:**1125–1140.
27. **Zhang, Z., and R. Zhang.** 2008. Proteasome activator PA28γ regulates p53 by enhancing its MDM2-mediated degradation. EMBO J. **27:**852–864.

Journal of Virology, Aug. 2009, p. 7959–7969 Vol. 83, No. 16
0022-538X/09/$08.00+0 doi:10.1128/JVI.00889-09
Copyright © 2009, American Society for Microbiology. All Rights Reserved.

Human VAP-C Negatively Regulates Hepatitis C Virus Propagation[▽]

Hiroshi Kukihara,[1] Kohji Moriishi,[1] Shuhei Taguwa,[1] Hideki Tani,[1] Takayuki Abe,[1] Yoshio Mori,[1] Tetsuro Suzuki,[2] Takasuke Fukuhara,[1,3] Akinobu Taketomi,[3] Yoshihiko Maehara,[3] and Yoshiharu Matsuura[1]*

Department of Molecular Virology, Research Institute for Microbial Diseases, Osaka University, Osaka,[1] Department of Virology II, National Institute of Infectious Diseases, Tokyo,[2] and Department of Surgery and Science, Graduate School of Medical Sciences, Kyushu University, Fukuoka,[3] Japan

Received 3 May 2009/Accepted 2 June 2009

Human vesicle-associated membrane protein-associated protein (VAP) subtype A (VAP-A) and subtype B (VAP-B) are involved in the regulation of membrane trafficking, lipid transport and metabolism, and the unfolded protein response. VAP-A and VAP-B consist of the major sperm protein (MSP) domain, the coiled-coil motif, and the C-terminal transmembrane anchor and form homo- and heterodimers through the transmembrane domain. VAP-A and VAP-B interact with NS5B and NS5A of hepatitis C virus (HCV) through the MSP domain and the coiled-coil motif, respectively, and participate in the replication of HCV. VAP-C is a splicing variant of VAP-B consisting of the N-terminal half of the MSP domain of VAP-B followed by the subtype-specific frameshift sequences, and its biological function has not been well characterized. In this study, we have examined the biological functions of VAP-C in the propagation of HCV. VAP-C interacted with NS5B but not with VAP-A, VAP-B, or NS5A in immunoprecipitation analyses, and the expression of VAP-C inhibited the interaction of NS5B with VAP-A or VAP-B. Overexpression of VAP-C impaired the RNA replication of the HCV replicon and the propagation of the HCV JFH1 strain, whereas overexpression of VAP-A and VAP-B enhanced the replication. Furthermore, the expression of VAP-C was observed in various tissues, whereas it was barely detected in the liver. These results suggest that VAP-C acts as a negative regulator of HCV propagation and that the expression of VAP-C may participate in the determination of tissue tropism of HCV propagation.

Hepatitis C virus (HCV) is a major causative agent of chronic liver disease and thus a major public health problem, infecting at least 3% of the world population (47). HCV infection proceeds to the persistent stage in approximately 80% of patients, leading to the development of cirrhosis in 20% to 50% of patients, of whom approximately 5% eventually develop hepatocellular carcinoma (12). HCV encompasses a single-stranded positive-sense RNA genome of approximately 9.6 kb, which encodes a large precursor polyprotein comprising approximately 3,000 amino acids (26). The structural proteins are cleaved from the N-terminal one-fourth of the polyprotein by the host signal peptidase and signal peptide peptidase (23, 32, 33), resulting in the maturation of the capsid protein, two envelope proteins and viroporin p7. The NS2 protease cleaves after the carboxyl terminus, and then NS3 cleaves the appropriate downstream positions to produce NS4A, NS4B, NS5A, and NS5B (8, 42), all of which form the replication complex along with several host proteins (5, 21). NS5B is the RNA-dependent RNA polymerase, which is a main enzymatic component of the replication complex of HCV (3), while NS5A is a membrane-anchored zinc-binding phosphoprotein that appears to possess diverse functions, including the suppression of host defense and the regulation of the virus's replication (1, 4, 6, 41), although its biological function remains unclear.

* Corresponding author. Mailing address: Department of Molecular Virology, Research Institute for Microbial Diseases, Osaka University, 3-1, Yamadaoka, Suita, Osaka 565-0871, Japan. Phone: 81-6-6879-8340. Fax: 81-6-6879-8269. E-mail: matsuura@biken.osaka-u.ac.jp.

▽ Published ahead of print on 10 June 2009.

The NS5A protein has been shown to interact with several host proteins, including vesicle-associated membrane protein (VAMP)-associated protein (VAP) subtype A (VAP-A) (44) and subtype B (VAP-B) (9), FKBP8 (34), MyD88 (1), FBL2 (46), human butyrate-induced transcript 1 (hB-ind1) (40), and so on (25). VAP-A and VAP-B also bind to NS5B, although it remains unclear whether these interactions modulate HCV replication positively or negatively (9, 44). VAP-A and VAP-B have been shown to associate with the cytoplasmic face of the endoplasmic reticulum (ER) and the Golgi apparatus (38) and to consist of the major sperm protein (MSP) domain, the coiled-coil domain, and the transmembrane (TM) region, in that order (30, 39), as shown in Fig. 1A. VAP was originally reported as a protein binding to VAMP, which is a synaptic vesicle SNARE protein required for synaptic-vesicle fusion in the nematode *Aplysia californica*, and was designated the 33-kDa VAMP-associated protein, VAP-33 (39). Two mammalian homologues, VAP-A and VAP-B, were subsequently identified (30, 38). The transcription of VAP-A and VAP-B is ubiquitously detected in mammalian organs, including the heart, placenta, lung, liver, skeletal muscle, and pancreas (30), suggesting that VAP family proteins are involved in diverse cellular functions other than neurotransmitter release (30, 38, 49). Several VAP-interacting proteins share the FFAT motif (two phenylalanines in an acidic tract), which has the consensus amino acid sequence EFFDAXE, as determined by a comparison among oxysterol binding proteins (OSBPs), OSBP-related proteins (ORPs) (20), and the ceramide transport protein CERT (10, 19), contributing to the regulation of fatty acid metabolism. The interaction of VAP family proteins with

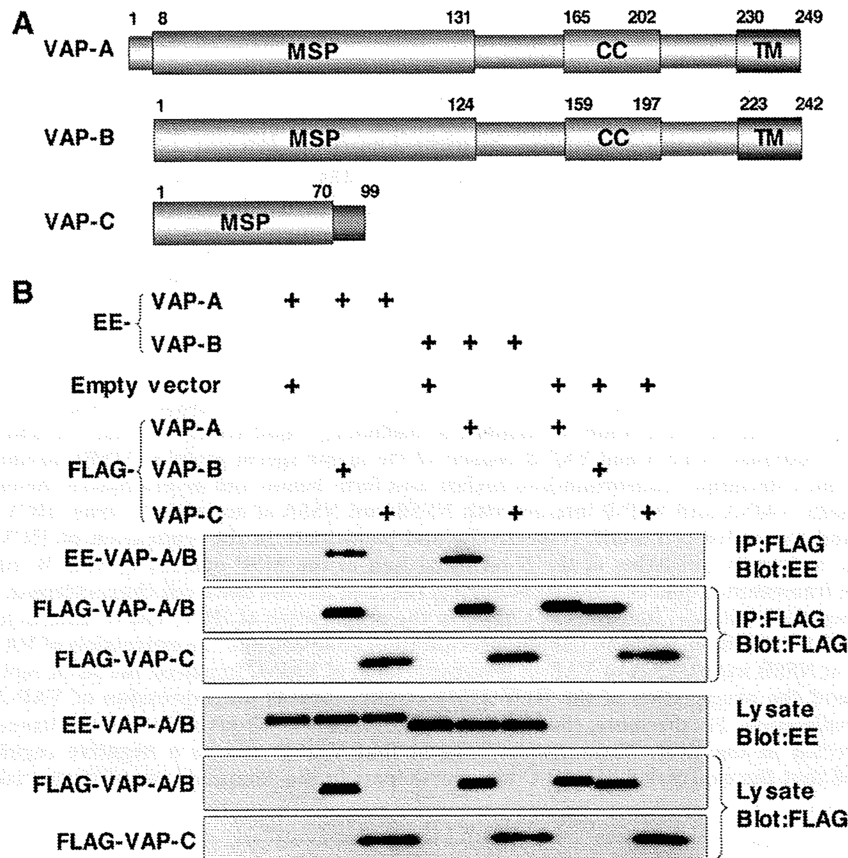

FIG. 1. VAP-C interacts with neither VAP-A nor VAP-B. (A) Structures of VAP family proteins. The MSP domain, the coiled-coil domain, and the TM region are indicated as MSP, CC, and TM, respectively. (B) Interaction among VAP family proteins. The expression plasmids encoding VAP proteins or empty vector (1 μg each) were transfected into 293T cells, FLAG-tagged VAP proteins coexpressed with EE-tagged VAP-A or VAP-B were immunoprecipitated (IP) with anti-FLAG antibody, and the resulting precipitates were examined by immunoblotting using anti-FLAG or anti-EE antibody. One percent of the volume of the lysate was used as an input control. The data in each panel are representative of the results of three independent experiments. +, present.

other host proteins, including VAMP and tubulin, is independent of the FFAT motif (16, 36, 38, 50). The third subtype of VAP is VAP-C, which is an alternative spliced isoform of VAP-B, consisting of the N-terminal half of the MSP domain and the subtype-specific 29 amino acids (Fig. 1A). However, its tissue distribution and physiological function remain largely unknown.

Glutathione *S*-transferase pulldown and immunoprecipitation analyses revealed that both VAP-A and VAP-B interact with NS5B and NS5A through the MSP domain and the coiled-coil domain, respectively (9, 44), and the MSP domains of VAP-A and VAP-B exhibit 82.3% homology. Although VAP-C possesses the N-terminal-half region of the MSP domain of VAP-B, the biological significance of VAP-C in the propagation of HCV has not yet been clarified. In this study, we examined the expression of VAP-C in human tissues and the effects of VAP-C expression on the RNA replication, translation, and particle formation of HCV.

MATERIALS AND METHODS

Cell lines. Cells of the human hepatoma cell line Huh-7, cell line Huh7OK1, and embryonic kidney cell line 293T were maintained in Dulbecco's modified Eagle's medium (DMEM) (Sigma, St. Louis, MO) containing 10% fetal calf serum (FCS) and nonessential amino acids (NEAA), while Huh 9-13 cells, which possess a subgenomic HCV RNA replicon of genotype 1b (21), were cultured in DMEM supplemented with 10% FCS, NEAA, and 1 mg/ml G418. The Huh7OK1 cell line exhibits the highest efficiency of propagation of strain JFH1 virus, as described previously (35). All cell lines were cultured at 37°C in a humidified atmosphere with 5% CO_2.

Antibodies. Chicken anti-human VAP-B antibody was described previously (9). Rabbit anti-human VAP-C antibody was prepared by immunization using synthetic peptides of the amino acid residues from 86 to 98, QPHFSISPNWEGR, which region does not share the homology to VAP-A and VAP-B. The mouse monoclonal antibody to human VAP-A was purchased from BD Pharmingen (San Diego, CA). Mouse monoclonal antibodies to influenza virus hemagglutinin (HA) and the GluGlu (EE) tag were from Covance (Richmond, CA). Mouse and rabbit anti-FLAG antibodies and mouse anti-β-actin monoclonal antibody were from Sigma. Rabbit polyclonal antibody to NS5A was prepared as described previously (34). Mouse anti-NS5A monoclonal antibody was from Austral Biologicals (San Ramon, CA).

Plasmids. A cDNA clone encoding NS5A was amplified from HCV genotype 1b strain J1 (9) (GenBank database accession number D89815) by PCR, using *Pfu* turbo DNA polymerase (Stratagene, La Jolla, CA). The fragments were then cloned into the appropriate sites in pEF-FLAG pGBK puro (13). The DNA fragment encoding NS5B of the J1 strain was generated by PCR and cloned into pCAGGs-PUR (31). The DNA fragment encoding human VAP-A was amplified by PCR from a human fetal-brain library (Clontech, Palo Alto, CA) and was introduced into pEF-FLAG pGBK puro and pEF-EE hygro (13), as described previously (9). A DNA fragment encoding VAP-C was amplified from cDNA of hepatoma cell line Huh-7 and was introduced into pEF-FLAG pGBK puro. Pro^{56}-to-Ser (P56S) mutants of VAPs were generated by site-directed mutagen-

esis (11). All PCR products were confirmed by sequencing with an ABI Prism 3130 genetic analyzer (Applied Biosystems, Tokyo, Japan).

Transfection, immunoblotting, and immunoprecipitation. Cells were seeded onto a six-well tissue culture plate 24 h before transfection. The plasmids were transfected into cells by liposome-mediated transfection using TransIT LT1 (Mirus Bio, Madison, WI). These transfected cells were harvested at 36 h posttransfection, washed three times with 1 ml of ice-cold phosphate-buffered saline (PBS), and suspended in 0.2 ml lysis buffer (20 mM Tris-HCl, pH 7.4, containing 135 mM NaCl and 1% Triton X-100) supplemented with protease inhibitor cocktail (Roche, Indianapolis, IN). The cell lysates were sonicated at 4°C for 5 min, incubated for 30 min at 4°C, and centrifuged at 15,000 rpm for 30 min at 4°C. The supernatant was subjected to immunoprecipitation analyses as described previously (27). The immunoprecipitated proteins were boiled in 30 μl of loading buffer and then subjected to sodium dodecyl sulfate–12.5% polyacrylamide gel electrophoresis. The proteins were transferred to polyvinylidene difluoride membranes (Millipore, Bedford, MA) and then reacted with primary antibody and secondary horseradish peroxidase-conjugated antibody. The immunocomplexes were visualized with Super Signal West Femto substrate (Pierce, Rockford, IL) and detected by using an LAS-3000 image analyzer (Fujifilm, Tokyo, Japan). The distribution of VAPs in human organs was determined by using premade human tissue lysates (Protein medleys; Clonetech), which are aliquots of various organ lysates prepared from samples from several people, and liver tissues obtained during surgery after approval of the ethical committee of Kyushu University Graduate School of Medicine.

Real-time PCR. The HCV genomic RNA was determined by the method described previously (40). Total RNA was prepared from cells by using an RNeasy mini kit (Qiagen, Tokyo, Japan). First-strand cDNA was synthesized using an RNA LA PCR kit (Takara Bio, Inc., Shiga, Japan) and random primers. Expression of the appropriate gene was estimated by using platinum SYBR green quantitative PCR SuperMix UDG (Invitrogen, Carlsbad, CA) according to the manufacturer's protocol. Fluorescent signals were estimated by using an ABI Prism 7000 system (Applied Biosystems). The 5′ untranslated region of HCV and the glyceraldehyde-3-phosphate dehydrogenase (GAPDH) mRNA were amplified using primer pairs described previously (40). The amount of HCV genomic RNA was normalized with that of GAPDH mRNA.

Focus-forming assay. The viral RNA of the JFH1 strain was introduced into the Huh7OK1 cell line according to the method of Zhong et al. (51). The culture supernatant was collected at 7 days posttransfection and used as the infectious HCV particles. Huh7OK1 cells in DMEM containing 10% FCS were seeded at 5×10^4 cells per well into a 24-well plate 12 h before infection. The cells were infected with the JFH1 strain at a multiplicity of infection (MOI) of 0.05 and incubated at 37°C for 2 h. The medium was replaced with fresh DMEM containing 10% FCS and NEAA at 2 h postinfection. The cells were fixed with 4% paraformaldehyde at 96 h postinfection and permeabilized with PBS containing 0.2% Triton X-100. These fixed and permeabilized cells were stained with the anti-NS5A mouse monoclonal antibody and Alexa Fluor (AF) 488-conjugated antibody to mouse immunoglobulin G (Molecular Probes, Eugene, OR). Clusters of infected cells stained with the NS5A antibody were derived from a single infectious focus, and virus titers were represented as focus-forming units/ml.

Quantification of the HCV core protein by ELISA. The HCV core protein was quantified by using an Ortho HCV antigen enzyme-linked immunosorbent assay (ELISA) test (Ortho Clinical Diagnostics, Tokyo, Japan) according to the manufacturer's instructions. To determine the intracellular expression of core protein, Huh7OK1 cells were infected with the infectious HCV particles described above, lysed with the lysis buffer on ice, and applied to the ELISA after 100- to 10,000-fold dilution with PBS. Total protein was quantified by using a Micro BCA protein assay reagent kit (Pierce). The intracellular and extracellular levels of expression of the core protein were normalized by the total amount of protein.

Effect of the VAP expression on the cap-independent translational activity of the viral IRES. The cDNA fragment encoding a firefly luciferase was excised from a pGL3 basic plasmid (Promega, Madison, WI) and introduced into the downstream region of the *Renilla* luciferase gene of pRL-CMV (cytomegalovirus) (Promega). Then, the cDNA fragments encoding the internal ribosome entry site (IRES) of the HCV strains Con1 and JFH1 were introduced between the *Renilla* and firefly luciferase genes, and the resulting plasmids were designated pRL-CMV-HCVCon1 and pRL-CMV-HCVJFH1, respectively (see Fig. 4A). The IRES region of HCV was replaced with that of poliovirus (PV) or encephalomyocarditis virus (EMCV), and the plasmids designated pRL-CMV-PV and pRL-CMV-EMCV, respectively (see Fig. 4B). Each reporter plasmid was introduced into Huh7OK1 cells that had been transfected with the expression plasmid encoding FLAG-green fluorescent protein (GFP), FLAG–VAP-A, FLAG–VAP-B, or FLAG–VAP-C 24 h previously, and cells were harvested at 48 h posttransfection. Luciferase activities in cells were measured by using a dual-luciferase reporter assay system (Promega). The activity of firefly luciferase was normalized with that of *Renilla* luciferase and represented as relative luciferase activity (RLU).

Indirect immunofluorescence assay. The Huh 9-13 cells were cultured on glass slides and transfected with the expression plasmids encoding FLAG-tagged VAPs, P56S VAP mutants, or empty vector. The resulting cells were fixed at 72 h posttransfection with 4% paraformaldehyde in PBS at room temperature for 30 min. After being washed twice with PBS, cells were permeabilized for 20 min at room temperature with PBS containing 0.25% saponin and blocked with PBS containing 1% bovine serum albumin (BSA-PBS) for 60 min at room temperature. The cells were then incubated with BSA-PBS containing rabbit anti-FLAG and mouse anti-NS5A antibodies at 37°C for 60 min, washed three times with PBS containing 1% Tween 20 (PBS-T), and incubated with BSA-PBS containing AF 488-conjugated goat anti-rabbit immunoglobulin G and AF 594-conjugated goat anti-mouse antibodies at 37°C for 60 min. Finally, the cells were washed three times with PBS-T and observed with a FluoView FV1000 laser-scanning confocal microscope (Olympus, Tokyo, Japan).

RESULTS

VAP-C interacts with neither VAP-A nor VAP-B. The length of VAP-A was originally reported to be 242 amino acids but was recently corrected to 249 amino acids in the GenBank database due to the detection of 7 extra amino acids in the N terminus (Fig. 1A). VAP-C is a splicing variant of VAP-B that shares the N-terminal half of the MSP domain with VAP-B but lacks the coiled-coil motif and TM region (Fig. 1A). The region spanning residues 71 to 99 of VAP-C exhibits no homology to VAP-A and VAP-B, due to the frameshift. VAP-A and VAP-B form homo- or heterodimers via their TM domains, which is required for HCV replication (9, 44). To examine whether VAP-C is capable of interacting with VAP-A and VAP-B, FLAG-tagged VAP-A, -B, or -C was coexpressed with EE-tagged VAP-A or -B in 293T cells and was immunoprecipitated with the anti-FLAG antibody. Although EE-tagged VAP-A and VAP-B were coprecipitated with FLAG-tagged VAP-B and VAP-A, as reported previously, FLAG–VAP-C was precipitated with neither EE–VAP-A nor EE–VAP-B (Fig. 1B). These results indicate that VAP-C does not interact with VAP-A and VAP-B.

VAP-C binds to NS5B and interrupts the interaction of VAP-A and VAP-B with NS5B. VAP-A and VAP-B were identified as NS5A-binding proteins by yeast two-hybrid screening (9, 44). The coiled-coil domains of VAP-A and VAP-B were involved in the binding to NS5A, contributing to the efficiency of HCV replication (9, 44). However, VAP-C does not have the coiled-coil domain (Fig. 1A) and, therefore, VAP-C was expected not to interact with NS5A. To examine whether or not interaction between VAP-C and NS5A actually occurred, HA-tagged NS5A was coexpressed with FLAG-tagged VAP-A, -B, or -C in 293T cells and was immunoprecipitated with anti-HA antibody (Fig. 2). The results showed that the expression level of FLAG–VAP-C in the transfected cells was comparable to that of FLAG–VAP-A or FLAG–VAP-B (Fig. 2A, left). Although FLAG-tagged VAP-A and VAP-B were coprecipitated with HA-NS5A, no precipitation of FLAG–VAP-C with NS5A was detected (Fig. 2A, right), indicating that VAP-C does not interact with NS5A.

The RNA-dependent RNA polymerase NS5B was shown to interact with VAP-A through the MSP domain (44). The region spanning residues 1 to 70 of VAP-C is the same as the N-terminal-half region of the MSP domain of VAP-B and exhibits 77% homology to that of VAP-A (Fig. 1A). To exam-

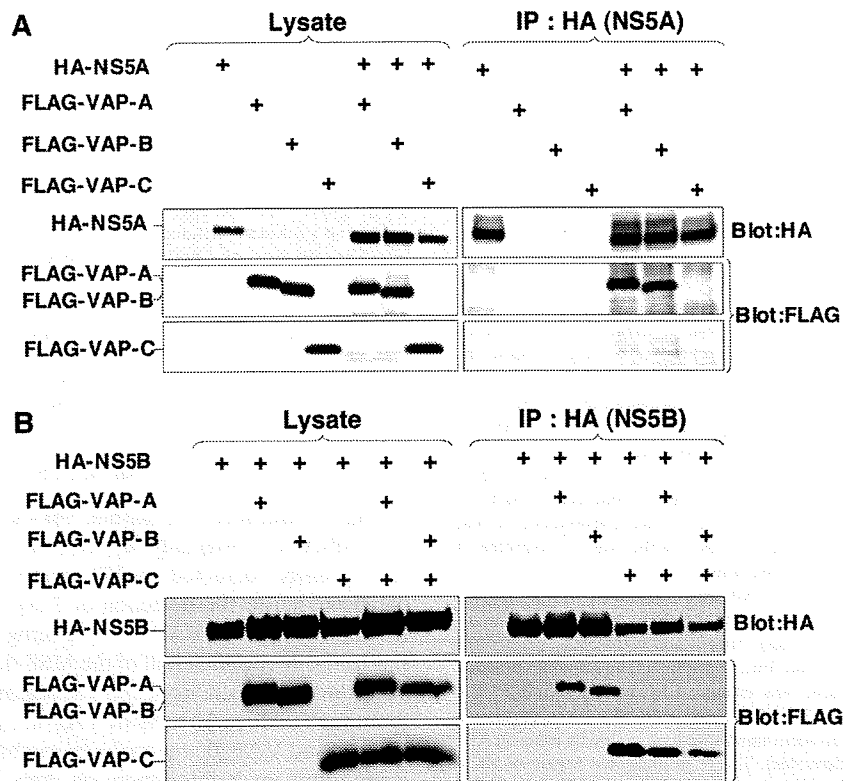

FIG. 2. VAP-C binds to NS5B but not NS5A and interrupts the interaction of VAP-A and VAP-B with NS5B. (A) The expression plasmids encoding NS5A or VAP proteins (1 μg each) were transfected into 293T cells after adjusting the total amounts of DNA to 2.0 μg with empty plasmid. HA-tagged NS5A was coexpressed with either FLAG-tagged VAP-A, VAP-B, or VAP-C in 293T cells and immunoprecipitated (IP) with anti-HA antibody, and the resulting precipitates were immunoblotted using anti-FLAG or anti-HA antibody. (B) The expression plasmids encoding NS5B or VAP proteins (1 μg each) were transfected into 293T cells after adjusting the total amounts of DNA to 3.0 μg with empty plasmid. HA-tagged NS5B was coexpressed with either FLAG-tagged VAP-A or VAP-B in the presence or absence of FLAG-tagged VAP-C in 293T cells and immunoprecipitated (IP) with anti-HA antibody, and the resulting precipitates were immunoblotted using anti-FLAG or anti-HA antibody. One percent of the lysate was used as an input control. The data in each panel are representative of the results of three independent experiments. +, present.

ine whether VAP-C is capable of interacting with NS5B, as are VAP-A and VAP-B, HA-NS5B was coexpressed with FLAG–VAP-A, FLAG–VAP-B, or FLAG–VAP-C in 293T cells and was immunoprecipitated with anti-HA antibody (Fig. 2B). Although substantial amounts of FLAG-tagged VAP-A, VAP-B, and VAP-C were coexpressed, and although all three were coprecipitated with HA-NS5B at comparable levels, the interaction of HA-NS5B with FLAG-tagged VAP-A or VAP-B was impaired by the coexpression of VAP-C, while FLAG–VAP-C was coprecipitated with HA-NS5B instead of FLAG-tagged VAP-A or VAP-B. These results suggest that VAP-C is capable of binding to NS5B and that the expression of VAP-C interrupts the interactions of NS5B with VAP-A and VAP-B.

Expression of VAP-C impairs the replication of HCV. VAP-A and VAP-B are known to support the replication of HCV RNA (2, 7). To examine the effect of VAP-C on the replication of HCV, FLAG–VAP-C was expressed in HCV replicon cells, Huh 9-13, in which a subgenomic HCV RNA of the genotype 1b strain Con1 was autonomously replicating. Huh 9-13 cells transfected with a plasmid encoding FLAG–VAP-C were harvested periodically up to 72 h posttransfection. The levels of replication of viral RNA and expression of NS5A were determined by real-time PCR and immunoblotting, respectively (Fig. 3). The expression of VAP-C reduced the intracellular RNA of the subgenomic HCV replicon in accordance with the incubation period after transfection with the expression plasmid of FLAG–VAP-C; the empty plasmid did not reduce the intracellular RNA (Fig. 3A). The expression of NS5A was gradually decreased and was undetectable at 72 h posttransfection, in contrast to the increase of VAP-C expression (Fig. 3B).

Next, to determine the effects of VAP-C expression on the replication of HCV, Huh 9-13 cells were transfected with 0 to 4 μg of the expression plasmid encoding VAP-A, VAP-B, or VAP-C and the replication of the subgenomic HCV RNA was determined at 48 h posttransfection. Although the HCV replicon cells transfected with 4 μg of a plasmid encoding FLAG–VAP-B exhibited enhancement of the RNA replication, those transfected with an equivalent amount of plasmid encoding FLAG–VAP-A or empty vector showed a slight reduction of HCV RNA replication. In contrast, the replicon cells transfected with a plasmid encoding FLAG–VAP-C exhibited a clear reduction of the HCV RNA replication in a dose-dependent manner (Fig. 3C). The expression of FLAG-tagged VAP-A, VAP-B, or VAP-C in the replicon cells was increased in correspondence with the amount of the transfected plasmid

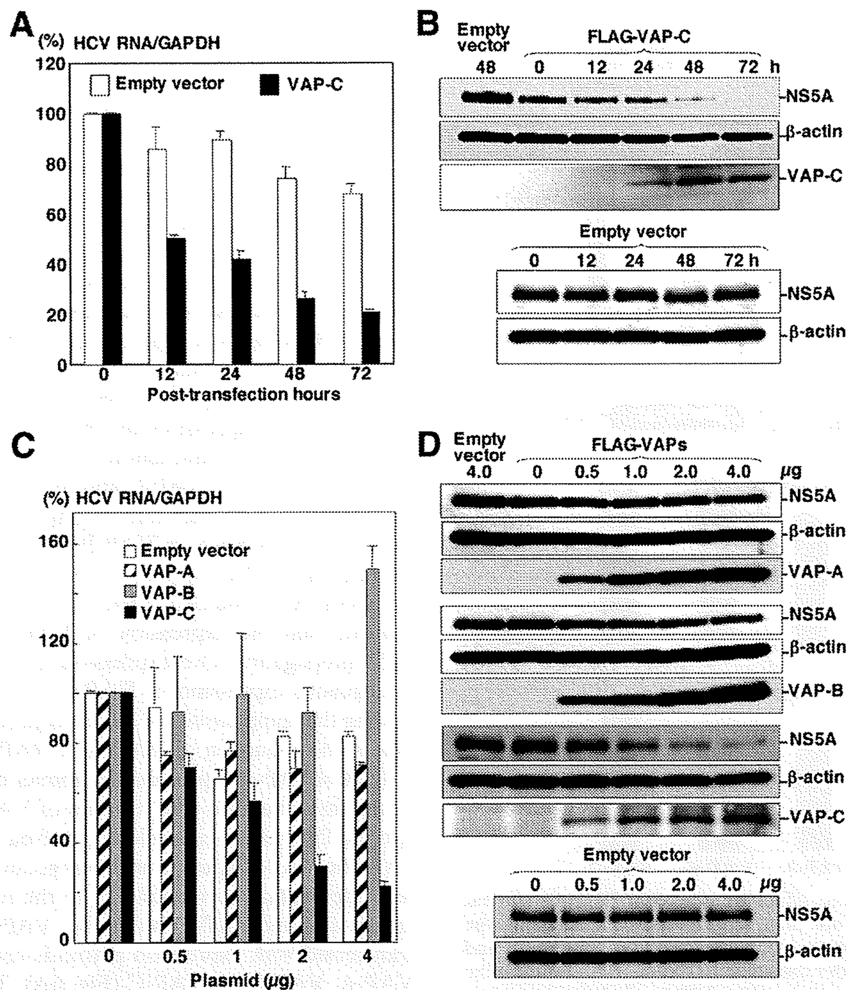

FIG. 3. Expression of VAP-C impairs the replication of HCV. (A) HCV replicon cells (Huh 9-13) were transfected with 4 μg of the expression plasmids encoding FLAG-tagged VAP-C or empty vector, and the level of intracellular HCV RNA was determined at 0, 12, 24, 48, or 72 h posttransfection by real-time PCR after normalization with GAPDH mRNA. The value of HCV RNA at 0 h posttransfection in the cell line transfected with the empty plasmid is represented as 100%. Data in this panel are shown as means ± standard deviations. (B) Huh 9-13 cells were transfected with 4 μg of the plasmid encoding FLAG-tagged VAP-C or empty plasmid, and the levels of expression of NS5A, β-actin, and VAP-C were determined at 0, 12, 24, 48, or 72 h posttransfection by immunoblotting using anti-NS5A, anti-β-actin, or anti-FLAG tag antibody. (C) Huh 9-13 cells were transfected with 0 to 4 μg of the plasmids encoding FLAG-tagged VAP-A, VAP-B, or VAP-C or empty vector, and the level of intracellular HCV RNA was determined at 72 h posttransfection as described for panel A. Data in this panel are shown as means ± standard deviations. (D) Huh 9-13 cells treated as described for panel C were harvested at 72 h posttransfection, and the levels of expression of NS5A, β-actin, VAP-A, VAP-B, and VAP-C were determined by immunoblotting. The data in each panel are representative of the results of three independent experiments.

(Fig. 3D), and the expression of NS5A was suppressed in accordance with the expression of FLAG–VAP-C, whereas the expression of FLAG–VAP-A and FLAG–VAP-B exhibited no effect on the expression of NS5A. These results suggest that the expression of VAP-C impairs the replication of HCV RNA.

VAP-C exhibits no effect on the IRES-dependent translation. The expression of VAP-C was shown to suppress the replication of the HCV RNA replication of the replicon cells. Next, to determine the effect of VAPs on the translation of HCV RNA, the reporter plasmid encoding the *Renilla* luciferase gene under the control of the CMV promoter and the firefly luciferase gene under the IRES of HCV, PV, or EMCV, in that order, was prepared as shown in Fig. 4. These reporter plasmids were introduced into Huh7OK1 cells 24 h after transfection of the expression plasmids encoding VAP-A, VAP-B, or VAP-C and harvested at 48 h posttransfection, and then the RLUs were determined. Although VAP-C exhibited a slight increase in the IRES-dependent translations of the HCV strains Con1 and JFH1, no significant effect of the expression of the VAPs on the HCV IRES-dependent translation was observed (Fig. 4A). Similarly, the expression of each of the VAPs in Huh7OK1 cells exhibited no significant effect on the IRES-dependent translation of PV or EMCV (Fig. 4B). These results indicate that the suppression of HCV RNA replication by the expression of

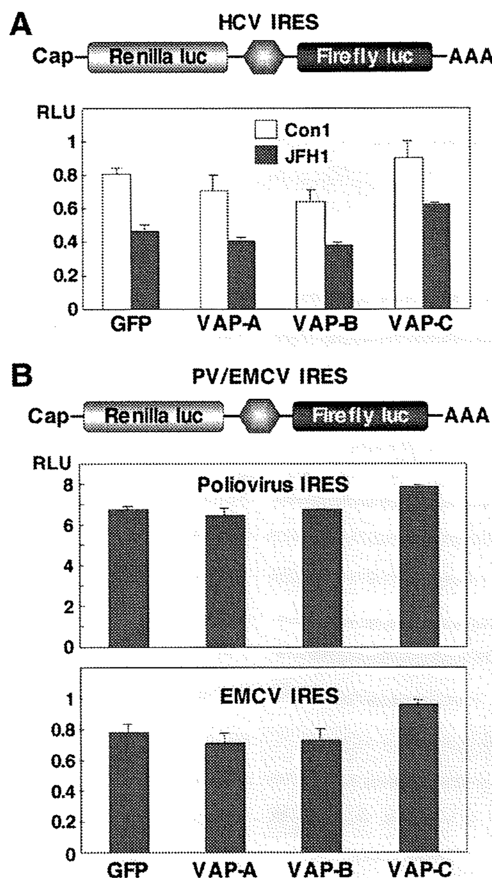

FIG. 4. VAP-C exhibits no effect on the viral IRES-dependent translation. (A) Top: structure of a reporter plasmid encoding the *Renilla* luciferase gene under the control of the CMV promoter and the firefly luciferase gene under the HCV IRES, in order. Bottom: the reporter plasmid was introduced into Huh7OK1 cells 24 h after transfection of the expression plasmids encoding VAP-A, VAP-B, or VAP-C, the cells harvested at 48 h posttransfection, and the RLUs determined after standardization with the expression of *Renilla* luciferase. (B) Top: structure of a reporter plasmid encoding the *Renilla* luciferase gene under the control of the CMV promoter and the firefly luciferase gene under the PV or EMCV IRES, in order. Bottom: each of the reporter plasmids was introduced into Huh7OK1 cells, and the RLU values were determined as described for panel A. Data in this figure are shown as the means ± standard deviations.

VAP-C was not due to the suppression of the IRES-dependent translation of the viral RNA genome.

VAP-C impairs HCV propagation. To examine the effect of VAP expression on HCV propagation, Huh7OK1 cells transfected with the expression plasmids encoding VAP-A, VAP-B, or VAP-C were infected with JFH1 virus, and the levels of production of the viral RNA, core protein, and infectious particles were determined at 96 h postinfection. The production of intracellular and extracellular viral RNA was increased up to 10 to 30 times and 2 to 3 times, respectively, by the expression of VAP-A or VAP-B whereas it was clearly decreased in a dose-dependent manner by the expression of VAP-C (Fig. 5A). Although the extracellular core protein was increased from 0.6 to 2.6 nmol/liter by the expression of VAP-A or VAP-B, as seen in the production of viral RNA, the intracellular core protein showed only a marginal increase (40 to 65 nmol/liter) (Fig. 5A). Although the reason for the discrepancy between the intracellular production of viral RNA and core protein is not known at the moment, some mechanisms other than RNA translation might be involved, because VAP expression exhibited no effect on the HCV IRES-dependent translation, as shown in Fig. 4A. In contrast to the enhancement of core protein production by the expression of VAP-A or VAP-B, the expression of VAP-C significantly reduced both the intracellular and extracellular expression of the core protein (Fig. 5A). Furthermore, the production of infectious particles in the culture supernatants of Huh7OK1 cells infected with JFH1 virus was slightly enhanced by the expression of VAP-A or VAP-B, whereas it was suppressed by the expression of VAP-C (Fig. 5A). To further confirm the effects of VAPs on the expression of HCV proteins, Huh7OK1 cells transfected with various amounts of the expression plasmids of VAP-A, VAP-B, or VAP-C and infected with the JFH1 virus were examined by immunoblotting (Fig. 5B). Although the expression of VAP-A or VAP-B exhibited no effect on NS5A expression, VAP-C expression clearly decreased the expression of NS5A in a dose-dependent manner. These results clearly indicate that the expression of VAP-C negatively regulates HCV propagation. Overexpression of VAP-C did not affect the endogenous expression of VAP-A or VAP-B (Fig. 5C), suggesting that suppression of HCV propagation by VAP-C is not due to the reduction of VAP-A or VAP-B expression.

Lack of VAP-C expression in human livers. VAP-C consists of the first 70 amino acid residues of VAP-B and the subtype-specific 29 amino acid residues derived from frameshift (Fig. 1A). The VAP-C-specific antibody generated by immunization with the peptide corresponding to the residues from 86 to 98 clearly detected VAP-C but neither VAP-A nor VAP-B in cells transfected with expression plasmids encoding FLAG-tagged VAP-A, VAP-B, or VAP-C (Fig. 6A). To determine the distribution of VAPs in human organs, the pool lysates of various organs prepared from several people were examined by immunoblotting (Fig. 6B). Expression of VAP-A was detected clearly in the kidney, lung, prostate, and liver; slightly in the duodenum, uterus, vagina, and bladder; and barely in the small intestine and stomach. VAP-B was detected clearly in the bladder, kidney, and prostate and slightly in the duodenum, small intestine, uterus, vagina, and liver. Expression of VAP-C was detected clearly in the stomach, uterus, kidney, and bladder; slightly in the duodenum, small intestine, and prostate; and barely detected in the vagina, lung, and liver. Several bands smaller than the expected size of VAP-C were observed in the stomach, duodenum, small intestine, uterus, vagina, prostate, and bladder. Because the main target of HCV replication is thought to be the liver, we next examined the expression of VAPs in individual human liver samples. VAP-A and VAP-B were clearly detected in the liver tissues obtained from chronic hepatitis C patients and a healthy donor, but no expression of VAP-C was detected (Fig. 6C). These results suggest that the expression of VAP-C may participate in the determination of tissue tropism of HCV propagation.

Substitution of Ser for Pro^{56} in VAPs leads to suppression of HCV replication. A single mutation of Pro^{56} to Ser (P56S) of VAP-B has been reported to be highly associated with amyotrophic lateral sclerosis (ALS), and the P56S mutation of VAP-B but not of VAP-A has been shown to induce large

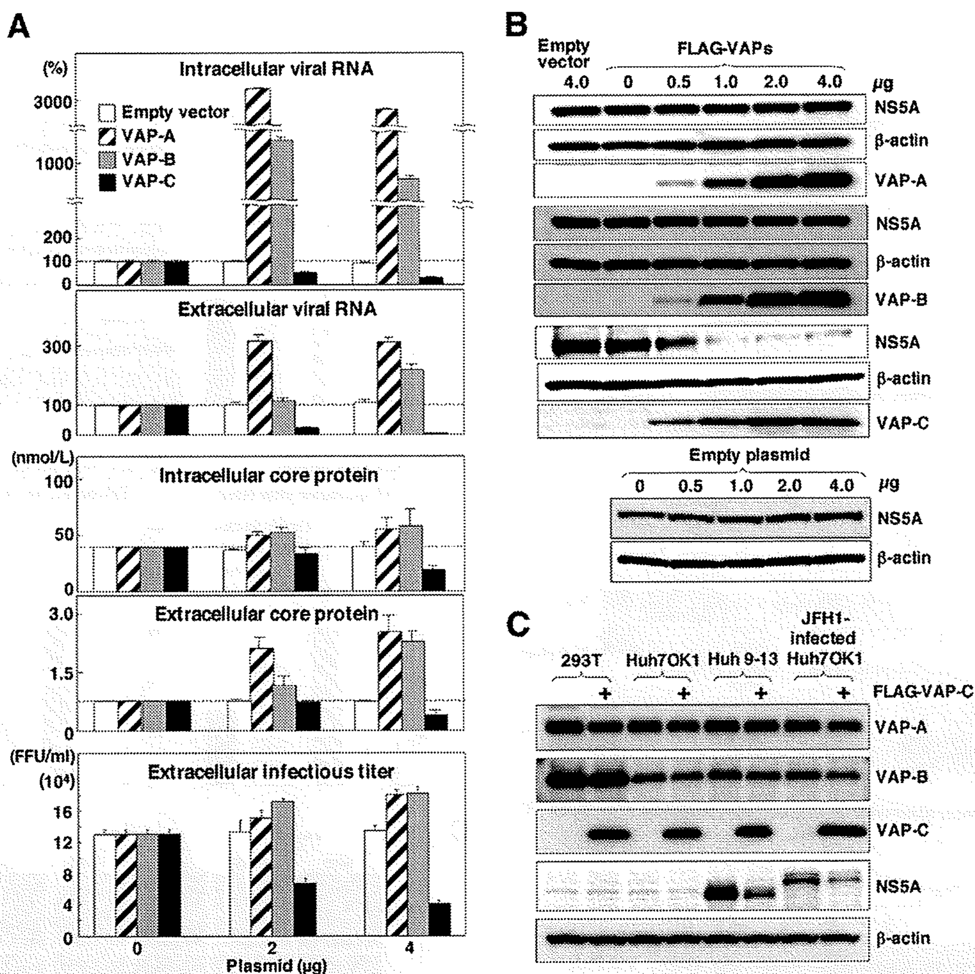

FIG. 5. VAP-C impairs HCV propagation but does not affect endogenous expression of VAP-A or VAP-B. Huh7OK1 cells transfected with 0 to 4 μg of plasmid encoding the FLAG-tagged VAP-A, VAP-B, or VAP-C or empty vector were infected with strain JFH1 at an MOI of 0.05 at 14 h posttransfection and then harvested at 96 h postinfection. (A) The intracellular and extracellular expression levels of viral RNA (top) and core protein (middle) were determined by real-time PCR and ELISA, respectively. Infectious viral titers in the culture supernatants were determined by focus-forming assay (bottom). Data in this panel are shown as the means ± standard deviations. (B) The expression levels of NS5A, β-actin, VAP-A, VAP-B, and VAP-C were determined by immunoblotting using anti-NS5A, anti-β-actin, or anti-FLAG tag antibody. (C) The embryonic kidney cell line (293T), the cured hepatoma cell line (Huh7OK1), and the replicon cell line (Huh 9-13) were transfected with 2 μg of the plasmid encoding FLAG-tagged VAP-C (+) or empty plasmid. In the case of the infected cells, Huh7OK1 cells were infected with strain JFH1 at an MOI of 0.05, reseeded onto the tissue culture plate at 96 h postinfection, and then transfected with 2 μg of the plasmids. These cells were harvested at 36 h posttransfection and examined by immunoblotting using antibodies to VAP-A, VAP-B, FLAG, NS5A, and β-actin. The data in each panel are representative of the results of three independent experiments.

aggregations of ER in culture cells and to sequester the wild-type protein into ubiquitinated inclusions (29, 37). To examine the effects on the replication of HCV of the P56S mutation in VAPs, FLAG-tagged VAP mutants were expressed in the HCV replicon cells. RNA replication of the subgenomic replicon in Huh 9-13 cells was impaired by the expression of each of the mutant VAPs (Fig. 7A, left). The expression of NS5A in the replicon cells was decreased by the expression of the mutant VAPs in a dose-dependent manner (Fig. 7A, right). Next, to examine the effect of the expression of the P56S VAP mutants on HCV propagation, Huh7OK1 cells expressing the FLAG-tagged VAP mutants were infected with JFH1 virus. The production of intracellular and extracellular viral RNA at 96 h postinfection was decreased by the expression of the P56S mutation in VAPs (Fig. 7B). Although the results of a previous study indicated that the expression of the P56S mutant of VAP-B but not that of VAP-A induced a large aggregation of ER in hamster ovary cell line CHO (37), the P56S mutants of VAP-A and VAP-B but not that of VAP-C exhibited accumulation of membranous aggregates in Huh 9-13 cells (Fig. 7C). These results indicate that the P56S mutation in both VAP-B and VAP-A induces aggregation of ER in human hepatoma cells, which in turn leads to the suppression of HCV propagation.

DISCUSSION

The replication of HCV has been shown to require several host proteins, including VAP-A/VAP-B (6, 9, 44), FBL2 (46), FKBP8 (34), hB-ind1 (40), Hsp90 (28, 34, 45), and cyclophilins

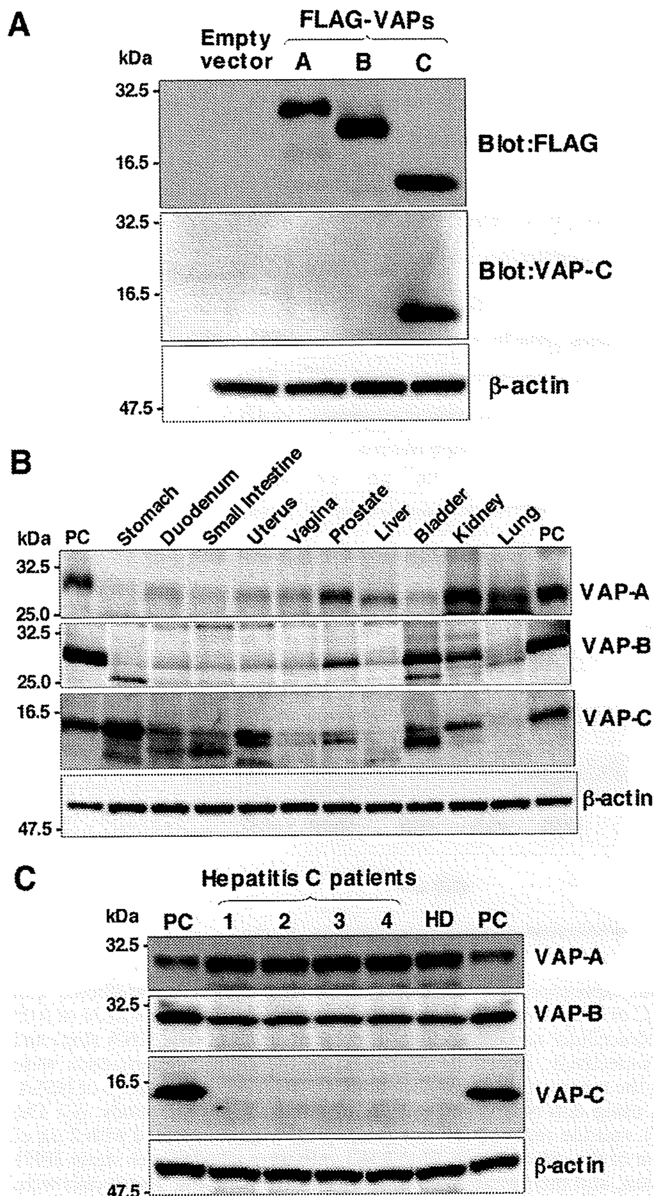

FIG. 6. Distribution of VAPs in human tissues. (A) Anti-VAP-C antibody specifically recognizes VAP-C. Human embryonic kidney 293T cells transfected with expression plasmid encoding FLAG-tagged VAP-A, VAP-B, or VAP-C or empty vector were harvested at 48 h posttransfection and examined by immunoblotting using anti-FLAG tag, anti-VAP-C, and anti-β-actin antibodies. (B) The premade human tissue lysates "Protein medleys" (20 μg each; Clonetech) were examined by immunoblotting using antibodies against VAP-A, VAP-B, VAP-C, or β-actin. (C) Expression of VAP family proteins in human liver tissues. Liver samples obtained from four hepatitis C patients (1 to 4) and one healthy donor (HD) were examined by immunoblotting as described above. The data in each panel are representative of the results of three independent experiments. PC indicates 293T cells transfected with expression plasmid encoding VAP-A, VAP-B, and VAP-C.

(15, 48). VAP-A has been detected in a detergent-resistant membrane fraction that was shown to be capable of replicating HCV RNA in vitro, and the interaction of VAP-A with NS5A is required for the efficient replication of HCV genomic RNA

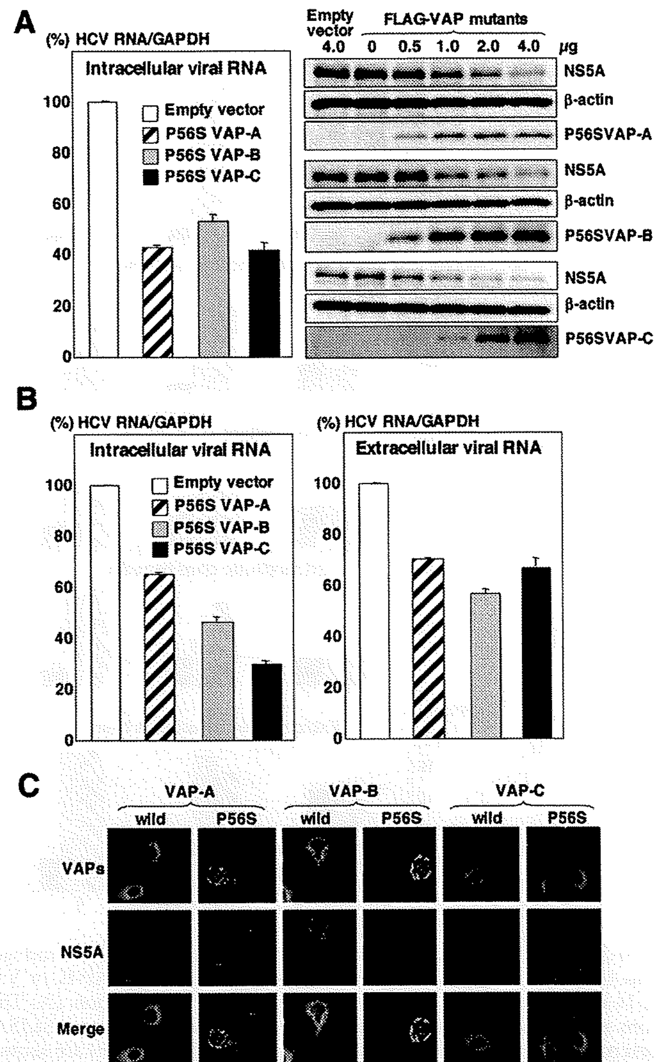

FIG. 7. Substitution of Ser for Pro^{56} in VAPs leads to suppression of HCV replication. (A) Left: Huh 9-13 cells were transfected with 4 μg of the expression plasmids encoding FLAG-tagged P56S VAP mutants or empty vector, and the level of intracellular HCV RNA was determined at 72 h posttransfection by real-time PCR after normalization with GAPDH mRNA. The value for HCV RNA at 0 h posttransfection in the cell line transfected with the empty plasmid is represented as 100%. Data in this panel are shown as the means ± standard deviations. Right: Huh 9-13 cells were transfected with 0 to 4 μg of the FLAG-tagged P56S VAP mutant plasmids or empty vector, and the levels of expression of NS5A, β-actin, and the mutant VAPs were determined by immunoblotting at 72 h posttransfection. The data in each panel are representative of the results of three independent experiments. (B) Huh7OK1 cells transfected with 4 μg of the expression plasmids encoding FLAG-tagged P56S VAP mutants or empty vector were infected with strain JFH1 at an MOI of 0.05 at 14 h posttransfection, and the intracellular (left) and extracellular (right) expression levels of viral RNA were determined by real-time PCR after normalization with GAPDH mRNA at 96 h postinfection. Data in this panel are shown as the means ± standard deviations. (C) Levels of expression of wild-type VAPs, P56S mutant VAPs, and NS5A in Huh 9-13 cells at 72 h after transfection with the expression plasmids encoding FLAG-tagged VAPs or P56S VAP mutants were determined by immunofluorescent assay. The data in each panel are representative of the results of three independent experiments.

(2, 7) and is modulated by the phosphorylation of NS5A (4, 6). VAP-B also participates in HCV replication through the formation of homo- and/or heterodimers with VAP-A (9). VAP-A and VAP-B form hetero- and homodimers through their TM regions and interact with NS5A and NS5B through the coiled-coil domain and MSP domain, respectively (9, 44). VAP-C is a splicing variant of VAP-B, consisting of the N-terminal half of VAP-B and the subtype-specific amino acid residues generated by the frameshift. However, the biological significance of VAP-C in the life cycle of HCV has not been determined. In this study, we have demonstrated that VAP-C is capable of binding to HCV NS5B but not to NS5A, VAP-A, and VAP-B due to the lack of the coiled-coil and TM regions. The expression of VAP-C inhibited the interaction of VAP-A and VAP-B with NS5B, impaired the RNA replication and particle formation of HCV, and was barely detected in human liver cells. These results suggest that VAP-C acts as a negative regulator for HCV propagation and is partly involved in the determination of the tissue specificity of HCV replication.

Overexpression of VAP-A but not of VAP-B inhibited the incorporation of the vesicular stomatitis virus (VSV) envelope glycoprotein G (VSV-G) into ER vesicles in CHO cells, resulting in impairment of membrane protein transport from the ER to the Golgi apparatus (37). VAP-B was shown to be involved in the unfolded protein response, which is an ER reaction to suppress the accumulation of misfolded proteins, and the expression of the P56S VAP-B mutant was suggested to nullify the unfolded protein response induced by VAP-B, to produce a large aggregation of ER, and to be involved in the development of ALS (17, 37). These data suggest that VAP-A and VAP-B possess different physiological functions; however, the contributions of the proteins to the life cycle of HCV have not been characterized. The expression of VAP-B but not of VAP-A resulted in an enhancement of the replication of the subgenomic HCV RNA of the genotype 1b strain Con1, whereas the expression of either VAP-A or VAP-B clearly enhanced viral RNA replication in cells infected with the genotype 2a strain JFH1 virus, suggesting that the contributions of VAP-A and VAP-B to viral RNA replication might differ among the genotypes of HCV. The expression of VAP-B or VAP-A enhanced RNA replication in the HCV replicon cells and the secretion of viral RNA, core protein, and infectious particles into the culture supernatants of Huh7OK1 cells infected with JFH1 virus, whereas the expression of these proteins had no effect on the expression of NS5A or on IRES-dependent translation. Thus, further studies will be needed to clarify the molecular mechanisms underlying the posttranslational enhancement of HCV production by the expression of VAP-A and VAP-B. In contrast to the expression of VAP-A and VAP-B, the expression of VAP-C clearly suppressed the RNA replication of both the genotype 1b RNA replicon cells and the genotype 2a strain JFH1 virus, by which both the expression of the viral proteins and the viral particle production were drastically impaired. Furthermore, the expression of the P56S mutants of VAP-A and VAP-B reduced RNA replication in HCV replicon cells and propagation of the JFH1 virus, probably due to the induction of aggregation of the ER. The reason why ER aggregation was induced by the expression of the P56S VAP-A mutant in Huh7 cells but not in CHO cells (17, 37) is not known at the moment.

The phosphorylation state of NS5A was suggested to control the interaction between VAP-A and NS5A and the replication efficiency of HCV RNA (6). Introduction of the adaptive mutations originally identified in the genotype 1b strain Con1 into NS5A of genotype 1a suppressed the hyperphosphorylation of NS5A, potentiated interaction with VAP-A, and enhanced the RNA replication (6). However, we have previously shown that NS5A of genotype 1a could bind to VAP-A and VAP-B at a level similar to that of genotype 1b despite the adaptive mutations (9). In this study, overexpression of each of the VAP proteins exhibited no effect on the mobility of NS5A in sodium dodecyl sulfate-polyacrylamide gel electrophoresis (Fig. 3 and 5), suggesting that there is no correlation between the VAP-dependent regulation of HCV propagation and the phosphorylation state of NS5A.

FKBP8 exhibits peptidyl prolyl *cis-trans* isomerase activity and interacts with NS5A and Hsp90 through the tetratricopeptide repeat (TPR) domain, and these interactions are suggested to be involved in the correct folding of the HCV replication complex (34). Treatment of cells with inhibitors of the ATPase activity of Hsp90, such as geldanamycin and its derivatives, impairs the RNA replication and particle production of HCV (28, 34, 45). The MSP domain of VAP-A was shown to interact with the TPR1 protein, which has a TPR domain and forms the chaperone complex with Hsp90 (22). Knockdown of the TPR1 protein or treatment with Hsp90 inhibitors in mammalian cells has been shown to inhibit the transport of VSV-G, leading to accumulation of the glycoprotein in the Golgi apparatus (22). The VAP-A- or VAP-B-induced enhancement of virus production might be attributable to the recruitment of Hsp90 into the replication complex through the interaction with the MSP domain.

VAP-A is well known to interact through the MSP domain with a number of mammalian and yeast proteins sharing the FFAT motif, including OSBPs, ORPs (20), and CERT (10, 19), and to be involved in the regulation of biosynthesis or trafficking of sterols and lipids. HCV replication and infection have been shown to be regulated by lipid components and to be capable of being inhibited by treatment with several inhibitors targeting lipid biosynthesis (14, 18). The intracellular membranous web structure observed in HCV replicon cells was shown to be resistant to detergent treatment, suggesting that the lipid raft-like structure abundant in cholesterol and sphingolipid is generated by the replication of HCV RNA (2, 24). Therefore, it might be feasible to speculate that VAP-A and VAP-B are involved in the construction of the HCV replication complex consisting of viral proteins and host cellular lipid components and that VAP-C interrupts the VAP-A and VAP-B functions and negatively regulates HCV propagation. Although the molecular mechanisms and the biological significance remain to be clarified, the MSP domain of VAP proteins was processed in human leukocytes and secreted into human serum (43). Further studies are needed to clarify the biogenesis and biological functions of the truncated VAP proteins in the replication of HCV.

In summary, we have shown that VAP-C is capable of suppressing the RNA replication and particle production of HCV by inhibiting the binding of VAP-A and VAP-B to NS5B through the N-terminal half of its MSP domain. The clear suppression of HCV propagation by the expression of VAP-C

further suggests the possibility of developing a novel therapeutic measure to eliminate HCV by the exogenous expression of VAP-C in the hepatocytes of chronic hepatitis C patients.

ACKNOWLEDGMENTS

We thank H. Murase for her secretarial work. We also thank R. Bartenschlager and T. Wakita for providing cell lines and plasmids.

This work was supported in part by grants-in-aid from the Ministry of Health, Labor, and Welfare; the Ministry of Education, Culture, Sports, Science, and Technology; the Global Center of Excellence Program; and the Foundation for Biomedical Research and Innovation.

REFERENCES

1. **Abe, T., Y. Kaname, I. Hamamoto, Y. Tsuda, X. Wen, S. Taguwa, K. Moriishi, O. Takeuchi, T. Kawai, T. Kanto, N. Hayashi, S. Akira, and Y. Matsuura.** 2007. Hepatitis C Virus nonstructural protein 5A modulates Toll-like receptor-MyD88-dependent signaling pathway in the macrophage cell lines. J. Virol. **81:**8953–8966.
2. **Aizaki, H., K. J. Lee, V. M. Sung, H. Ishiko, and M. M. Lai.** 2004. Characterization of the hepatitis C virus RNA replication complex associated with lipid rafts. Virology **324:**450–461.
3. **Behrens, S. E., L. Tomei, and R. De Francesco.** 1996. Identification and properties of the RNA-dependent RNA polymerase of hepatitis C virus. EMBO J. **15:**12–22.
4. **Blight, K. J., A. A. Kolykhalov, and C. M. Rice.** 2000. Efficient initiation of HCV RNA replication in cell culture. Science **290:**1972–1974.
5. **Egger, D., B. Wolk, R. Gosert, L. Bianchi, H. E. Blum, D. Moradpour, and K. Bienz.** 2002. Expression of hepatitis C virus proteins induces distinct membrane alterations including a candidate viral replication complex. J. Virol. **76:**5974–5984.
6. **Evans, M. J., C. M. Rice, and S. P. Goff.** 2004. Phosphorylation of hepatitis C virus nonstructural protein 5A modulates its protein interactions and viral RNA replication. Proc. Natl. Acad. Sci. USA **101:**13038–13043.
7. **Gao, L., H. Aizaki, J.-W. He, and M. M. C. Lai.** 2004. Interactions between viral nonstructural proteins and host protein hVAP-33 mediate the formation of hepatitis C virus RNA replication complex on lipid raft. J. Virol. **78:**3480–3488.
8. **Grakoui, A., D. W. McCourt, C. Wychowski, S. M. Feinstone, and C. M. Rice.** 1993. Characterization of the hepatitis C virus-encoded serine proteinase: determination of proteinase-dependent polyprotein cleavage sites. J. Virol. **67:**2832–2843.
9. **Hamamoto, I., Y. Nishimura, T. Okamoto, H. Aizaki, M. Liu, Y. Mori, T. Abe, T. Suzuki, M. M. Lai, T. Miyamura, K. Moriishi, and Y. Matsuura.** 2005. Human VAP-B is involved in hepatitis C virus replication through interaction with NS5A and NS5B. J. Virol. **79:**13473–13482.
10. **Hanada, K., K. Kumagai, S. Yasuda, Y. Miura, M. Kawano, M. Fukasawa, and M. Nishijima.** 2003. Molecular machinery for non-vesicular trafficking of ceramide. Nature **426:**803–809.
11. **Ho, S. N., H. D. Hunt, R. M. Horton, J. K. Pullen, and L. R. Pease.** 1989. Site-directed mutagenesis by overlap extension using the polymerase chain reaction. Gene **77:**51–59.
12. **Hoofnagle, J. H.** 2002. Course and outcome of hepatitis C. Hepatology **36:**S21–S29.
13. **Huang, D. C., S. Cory, and A. Strasser.** 1997. Bcl-2, Bcl-XL and adenovirus protein E1B19kD are functionally equivalent in their ability to inhibit cell death. Oncogene **14:**405–414.
14. **Ikeda, M., K. Abe, M. Yamada, H. Dansako, K. Naka, and N. Kato.** 2006. Different anti-HCV profiles of statins and their potential for combination therapy with interferon. Hepatology **44:**117–125.
15. **Inoue, K., T. Umehara, U. T. Ruegg, F. Yasui, T. Watanabe, H. Yasuda, J. M. Dumont, P. Scalfaro, M. Yoshiba, and M. Kohara.** 2007. Evaluation of a cyclophilin inhibitor in hepatitis C virus-infected chimeric mice in vivo. Hepatology **45:**921–928.
16. **Kaiser, S. E., J. H. Brickner, A. R. Reilein, T. D. Fenn, P. Walter, and A. T. Brunger.** 2005. Structural basis of FFAT motif-mediated ER targeting. Structure **13:**1035–1045.
17. **Kanekura, K., I. Nishimoto, S. Aiso, and M. Matsuoka.** 2006. Characterization of amyotrophic lateral sclerosis-linked P56S mutation of vesicle-associated membrane protein-associated protein B (VAPB/ALS8). J. Biol. Chem. **281:**30223–30233.
18. **Kapadia, S. B., and F. V. Chisari.** 2005. Hepatitis C virus RNA replication is regulated by host geranylgeranylation and fatty acids. Proc. Natl. Acad. Sci. USA **102:**2561–2566.
19. **Kawano, M., K. Kumagai, M. Nishijima, and K. Hanada.** 2006. Efficient trafficking of ceramide from the endoplasmic reticulum to the Golgi apparatus requires a VAMP-associated protein-interacting FFAT motif of CERT. J. Biol. Chem. **281:**30279–30288.
20. **Loewen, C. J., A. Roy, and T. P. Levine.** 2003. A conserved ER targeting motif in three families of lipid binding proteins and in Opi1p binds VAP. EMBO J. **22:**2025–2035.
21. **Lohmann, V., F. Korner, J. Koch, U. Herian, L. Theilmann, and R. Bartenschlager.** 1999. Replication of subgenomic hepatitis C virus RNAs in a hepatoma cell line. Science **285:**110–113.
22. **Lotz, G. P., A. Brychzy, S. Heinz, and W. M. Obermann.** 2008. A novel HSP90 chaperone complex regulates intracellular vesicle transport. J. Cell Sci. **121:**717–723.
23. **McLauchlan, J., M. K. Lemberg, G. Hope, and B. Martoglio.** 2002. Intramembrane proteolysis promotes trafficking of hepatitis C virus core protein to lipid droplets. EMBO J. **21:**3980–3988.
24. **Miyanari, Y., M. Hijikata, M. Yamaji, M. Hosaka, H. Takahashi, and K. Shimotohno.** 2003. Hepatitis C virus non-structural proteins in the probable membranous compartment function in viral genome replication. J. Biol. Chem. **278:**50301–50308.
25. **Moriishi, K., and Y. Matsuura.** 2007. Host factors involved in the replication of hepatitis C virus. Rev. Med. Virol. **17:**343–354.
26. **Moriishi, K., and Y. Matsuura.** 2003. Mechanisms of hepatitis C virus infection. Antivir. Chem. Chemother. **14:**285–297.
27. **Moriishi, K., T. Okabayashi, K. Nakai, K. Moriya, K. Koike, S. Murata, T. Chiba, K. Tanaka, R. Suzuki, T. Suzuki, T. Miyamura, and Y. Matsuura.** 2003. Proteasome activator PA28gamma-dependent nuclear retention and degradation of hepatitis C virus core protein. J. Virol. **77:**10237–10249.
28. **Nakagawa, S., T. Umehara, C. Matsuda, S. Kuge, M. Sudoh, and M. Kohara.** 2007. Hsp90 inhibitors suppress HCV replication in replicon cells and humanized liver mice. Biochem. Biophys. Res. Commun. **353:**882–888.
29. **Nishimura, A. L., M. Mitne-Neto, H. C. Silva, A. Richieri-Costa, S. Middleton, D. Cascio, F. Kok, J. R. Oliveira, T. Gillingwater, J. Webb, P. Skehel, and M. Zatz.** 2004. A mutation in the vesicle-trafficking protein VAPB causes late-onset spinal muscular atrophy and amyotrophic lateral sclerosis. Am. J. Hum. Genet. **75:**822–831.
30. **Nishimura, Y., M. Hayashi, H. Inada, and T. Tanaka.** 1999. Molecular cloning and characterization of mammalian homologues of vesicle-associated membrane protein-associated (VAMP-associated) proteins. Biochem. Biophys. Res. Commun. **254:**21–26.
31. **Niwa, H., K. Yamamura, and J. Miyazaki.** 1991. Efficient selection for high-expression transfectants with a novel eukaryotic vector. Gene **108:**193–199.
32. **Okamoto, K., Y. Mori, Y. Komoda, T. Okamoto, M. Okochi, M. Takeda, T. Suzuki, K. Moriishi, and Y. Matsuura.** 2008. Intramembrane processing by signal peptide peptidase regulates the membrane localization of hepatitis C virus core protein and viral propagation. J. Virol. **82:**8349–8361.
33. **Okamoto, K., K. Moriishi, T. Miyamura, and Y. Matsuura.** 2004. Intramembrane proteolysis and endoplasmic reticulum retention of hepatitis C virus core protein. J. Virol. **78:**6370–6380.
34. **Okamoto, T., Y. Nishimura, T. Ichimura, K. Suzuki, T. Miyamura, T. Suzuki, K. Moriishi, and Y. Matsuura.** 2006. Hepatitis C virus RNA replication is regulated by FKBP8 and Hsp90. EMBO J. **25:**5015–5025.
35. **Okamoto, T., H. Omori, Y. Kaname, T. Abe, Y. Nishimura, T. Suzuki, T. Miyamura, T. Yoshimori, K. Moriishi, and Y. Matsuura.** 2008. A single-amino-acid mutation in hepatitis C virus NS5A disrupting FKBP8 interaction impairs viral replication. J. Virol. **82:**3480–3489.
36. **Pennetta, G., P. R. Hiesinger, R. Fabian-Fine, I. A. Meinertzhagen, and H. J. Bellen.** 2002. Drosophila VAP-33A directs bouton formation at neuromuscular junctions in a dosage-dependent manner. Neuron **35:**291–306.
37. **Prosser, D. C., D. Tran, P. Y. Gougeon, C. Verly, and J. K. Ngsee.** 2008. FFAT rescues VAPA-mediated inhibition of ER-to-Golgi transport and VAPB-mediated ER aggregation. J. Cell Sci. **121:**3052–3061.
38. **Skehel, P. A., R. Fabian-Fine, and E. R. Kandel.** 2000. Mouse VAP33 is associated with the endoplasmic reticulum and microtubules. Proc. Natl. Acad. Sci. USA **97:**1101–1106.
39. **Skehel, P. A., K. C. Martin, E. R. Kandel, and D. Bartsch.** 1995. A VAMP-binding protein from *Aplysia* required for neurotransmitter release. Science **269:**1580–1583.
40. **Taguwa, S., T. Okamoto, T. Abe, Y. Mori, T. Suzuki, K. Moriishi, and Y. Matsuura.** 2008. Human butyrate-induced transcript 1 interacts with hepatitis C virus NS5A and regulates viral replication. J. Virol. **82:**2631–2641.
41. **Tellinghuisen, T. L., J. Marcotrigiano, and C. M. Rice.** 2005. Structure of the zinc-binding domain of an essential component of the hepatitis C virus replicase. Nature **435:**374–379.
42. **Tomei, L., C. Failla, E. Santolini, R. De Francesco, and N. La Monica.** 1993. NS3 is a serine protease required for processing of hepatitis C virus polyprotein. J. Virol. **67:**4017–4026.
43. **Tsuda, H., S. M. Han, Y. Yang, C. Tong, Y. Q. Lin, K. Mohan, C. Haueter, A. Zoghbi, Y. Harati, J. Kwan, M. A. Miller, and H. J. Bellen.** 2008. The amyotrophic lateral sclerosis 8 protein VAPB is cleaved, secreted, and acts as a ligand for Eph receptors. Cell **133:**963–977.
44. **Tu, H., L. Gao, S. T. Shi, D. R. Taylor, T. Yang, A. K. Mircheff, Y. Wen, A. E. Gorbalenya, S. B. Hwang, and M. M. Lai.** 1999. Hepatitis C virus RNA polymerase and NS5A complex with a SNARE-like protein. Virology **263:**30–41.

45. **Ujino, S., S. Yamaguchi, K. Shimotohno, and H. Takaku.** 2009. Heat-shock protein 90 is essential for stabilization of the hepatitis C virus non-structural protein NS3. J. Biol. Chem. **284:**6841–6846.
46. **Wang, C., M. Gale, Jr., B. C. Keller, H. Huang, M. S. Brown, J. L. Goldstein, and J. Ye.** 2005. Identification of FBL2 as a geranylgeranylated cellular protein required for hepatitis C virus RNA replication. Mol. Cell **18:**425–434.
47. **Wasley, A., and M. J. Alter.** 2000. Epidemiology of hepatitis C: geographic differences and temporal trends. Semin. Liver Dis. **20:**1–16.
48. **Watashi, K., N. Ishii, M. Hijikata, D. Inoue, T. Murata, Y. Miyanari, and K. Shimotohno.** 2005. Cyclophilin B is a functional regulator of hepatitis C virus RNA polymerase. Mol. Cell **19:**111–122.
49. **Weir, M. L., A. Klip, and W. S. Trimble.** 1998. Identification of a human homologue of the vesicle-associated membrane protein (VAMP)-associated protein of 33 kDa (VAP-33): a broadly expressed protein that binds to VAMP. Biochem. J. **333:**247–251.
50. **Weir, M. L., H. Xie, A. Klip, and W. S. Trimble.** 2001. VAP-A binds promiscuously to both v- and tSNAREs. Biochem. Biophys. Res. Commun. **286:**616–621.
51. **Zhong, J., P. Gastaminza, G. Cheng, S. Kapadia, T. Kato, D. R. Burton, S. F. Wieland, S. L. Uprichard, T. Wakita, and F. V. Chisari.** 2005. Robust hepatitis C virus infection in vitro. Proc. Natl. Acad. Sci. USA **102:**9294–9299.

Oxidative Stress Induces Anti-Hepatitis C Virus Status via the Activation of Extracellular Signal-Regulated Kinase

Masahiko Yano,[1,3] Masanori Ikeda,[1] Ken-ichi Abe,[1] Yoshinari Kawai,[1,2] Misao Kuroki,[1] Kyoko Mori,[1] Hiromichi Dansako,[1] Yasuo Ariumi,[1] Shougo Ohkoshi,[3] Yutaka Aoyagi,[3] and Nobuyuki Kato[1]

Recently, we reported that β-carotene, vitamin D_2, and linoleic acid inhibited hepatitis C virus (HCV) RNA replication in hepatoma cells. Interestingly, in the course of the study, we found that the antioxidant vitamin E negated the anti-HCV activities of these nutrients. These results suggest that the oxidative stress caused by the three nutrients is involved in their anti-HCV activities. However, the molecular mechanism by which oxidative stress induces anti-HCV status remains unknown. Oxidative stress is also known to activate extracellular signal-regulated kinase (ERK). Therefore, we hypothesized that oxidative stress induces anti-HCV status via the mitogen activated protein kinase (MAPK)/ERK kinase (MEK)–ERK1/2 signaling pathway. In this study, we found that the MEK1/2-specific inhibitor U0126 abolished the anti-HCV activities of the three nutrients in a dose-dependent manner. Moreover, U0126 significantly attenuated the anti-HCV activities of polyunsaturated fatty acids, interferon-γ, and cyclosporine A, but not statins. We further demonstrated that, with the exception of the statins, all of these anti-HCV nutrients and reagents actually induced activation of the MEK–ERK1/2 signaling pathway, which was inhibited or reduced by treatment not only with U0126 but also with vitamin E. We also demonstrated that phosphorylation of ERK1/2 by cyclosporine A was attenuated with *N*-acetylcysteine treatment and led to the negation of inhibition of HCV RNA replication. We propose that a cellular process that follows ERK1/2 phosphorylation and is specific to oxidative stimulation might lead to down-regulation of HCV RNA replication. *Conclusion:* Our results demonstrate the involvement of the MEK–ERK1/2 signaling pathway in the anti-HCV status induced by oxidative stress in a broad range of anti-HCV reagents. This intracellular modulation is expected to be a therapeutic target for the suppression of HCV RNA replication. (HEPATOLOGY 2009;50: 678-688.)

Hepatitis C virus (HCV), which belongs to the family Flaviviridae, is a single-stranded positive-sense RNA virus of approximately 9.6 kb.[1,2] Persistent infection with HCV causes chronic hepatitis, which often leads to liver cirrhosis and hepatocellular carcinoma.[3] Therefore, HCV infection is a major health problem worldwide. Interferon (IFN)-based therapies, including the combination of pegylated IFN with ribavirin, are the current standard strategies for chronic hepatitis, but their sustained virological response rates are unsatisfactory.[4,5] There is thus an urgent need for novel partners with IFN or more effective reagents that may improve the sustained virological response rate.

Following the development in 1999 of a cell culture system to support efficient HCV RNA replication,[6] numerous studies have identified reagents that inhibit HCV RNA replication and enhance the effect of IFN treatment.[7-9] Some of these reagents are already available for clinical use. Previously, we also developed a genome-length HCV RNA (strain O of genotype 1b) replication system (OR6) with Renilla luciferase (RL) as a reporter in hepatoma cell lines.[10] Using this OR6 assay system, we found that mizoribine,[11] as an immunosuppressant, and

Abbreviations: AA, arachidonic acid; BC, β-carotene; CsA, cyclosporine A; CyPA, cyclophilin A; DHA, docosahexaenoic acid; DMSO, dimethyl sulfoxide; EGF, epidermal growth factor: EPA, eicosapentaenoic acid; ERK, extracellular signal-regulated kinase; FBS, fetal bovine serum; FLV, fluvastatin; HCV, hepatitis C virus; IFN, interferon; LA, linoleic acid: MAPK, mitogen-activated protein kinase; MEK, MAPK/ERK kinase; NS5A, nonstructural 5A; PTV, pitavastatin; PUFA, polyunsaturated fatty acid; RL, renilla luciferase; ROS, reactive oxygen species; VD2, vitamin D_2; VE, vitamin E.

From the Departments of [1]Tumor Virology and [2]Gastroenterology and Hepatology, Okayama University Graduate School of Medicine, Dentistry, and Pharmaceutical Sciences, Okayama, Japan; and the [3]Division of Gastroenterology and Hepatology, Graduate School of Medical and Dental Sciences, Niigata University, Niigata City, Japan.

Received August 5, 2008; accepted April 8, 2009.

Supported by grants-in-aid for a third-term comprehensive 10-year strategy for cancer control and for research on hepatitis from the Ministry of Health, Labor, and Welfare of Japan. K. A. was supported by a Research Fellowship from the Japan Society for the Promotion of Science for Young Scientists.

Address reprint requests to: Masanori Ikeda, Department of Tumor Virology, Okayama University Graduate School of Medicine, Dentistry, and Pharmaceutical Sciences, 2-5-1 Shikata-cho, Okayama 700-8558, Japan. E-mail: maikeda@md.okayama-u.ac.jp; fax: (81)-86-235-7392.

Copyright © 2009 by the American Association for the Study of Liver Diseases.

Published online in Wiley InterScience (www.interscience.wiley.com).

DOI 10.1002/hep.23026

Potential conflicts of interest: Nothing to report.

Additional Supporting Information may be found in the online version of this article.

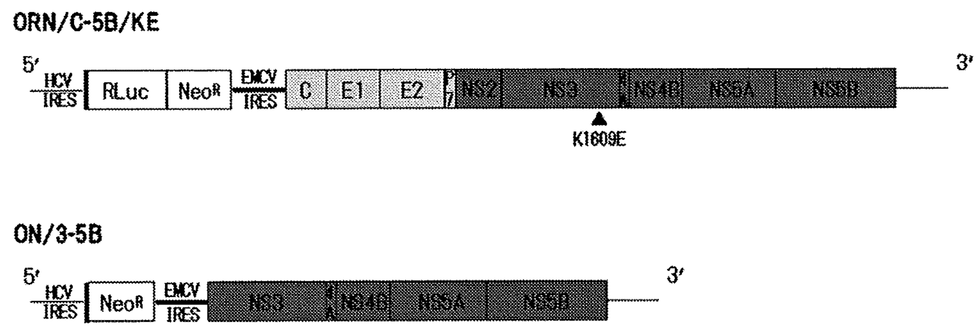

Fig. 1. Schematic gene organization of the genome-length and subgenomic HCV RNA used in this study. ORN/C-5B/KE encoding the RL gene was replicated in OR6 cells and ON/3-5B in sO cells. RL in OR6 cells was expressed as a fusion protein with neomycin phosphotransferase (Neo^R). The arrowhead indicates the position of K1609E, an adaptive mutation.

fluvastatin (FLV) and pitavastatin (PTV),[9-12] as the reagents for hypercholesterolemia, suppressed genome-length HCV RNA replication. Furthermore, in a recent study[13] in which we comprehensively analyzed the activities of ordinary nutrients on HCV RNA replication, three nutrients, β-carotene (BC), vitamin D_2 (VD2), and linoleic acid (LA), were found to suppress HCV RNA replication and enhance the antiviral activity of IFN-α or cyclosporine A (CsA) in an additive or a synergistic manner. Because the anti-HCV activities of these three nutrients, as well as CsA, were canceled by treatment with antioxidants such as vitamin E (VE) or selenium, we suggested that oxidative stress might be involved in the anti-HCV activities of these three nutrients and CsA. However, the detailed molecular mechanism via which the oxidative effects of these three nutrients and CsA suppress HCV RNA replication has not been explored.

The production of reactive oxygen species (ROS) plays a pivotal role in various cellular processes, including cell proliferation, differentiation, and apoptosis.[14] Whereas high-level production of ROS resulting from external stimuli is recognized as an important component of the pathogenesis of inflammatory and cancerous diseases, endogenously produced ROS at low concentrations are shown to function as signaling mediators of cellular responses.[15,16] Emerging evidence indicates that these ROS-triggered responses are mediated primarily via cellular signaling cascades, including a signaling pathway of extracellular signal-regulated kinase (ERK)1/2, namely p44/42 mitogen-activated protein kinase (MAPK), which belongs to the MAPK family.[17,18]

Several studies have revealed that certain viral proteins initiate activation of the MAPK/ERK kinase (MEK)–ERK1/2 signaling pathway, which may facilitate the viral replication and infectivity in the infected cells.[19,20] The HCV core protein[21] and the envelope protein[22] have also been reported to up-regulate this signaling pathway. However, another study reported that the HCV non-structural 5A (NS5A) protein suppressed activating protein-1 activation by inhibiting the phosphorylation of ERK1/2 in replicon cells.[23] Moreover, recent studies using an inhibitor specific to the MEK–ERK1/2 signaling pathway reported that the direct anti-HCV activities of IFN-γ[24] and acetylsalicylic acid[25] are mediated in part through the induction of this cascade.

We demonstrate that the activation of MEK–ERK1/2 signaling plays a significant role in the anti-HCV activity caused by oxidative stress in a broad range of anti-HCV reagents.

Materials and Methods

Reagents and Antibodies. Dimethyl sulfoxide (DMSO), BC, VD2, VE, LA, arachidonic acid (AA), eicosapentaenoic acid (EPA), docosahexaenoic acid (DHA), and IFN-γ were purchased from Sigma Aldrich (St. Louis, MO), and CsA, FLV, U0126, PD98059, SB203580, and c-Jun N-terminal kinase inhibitor II were obtained from Calbiochem (San Diego, CA). Epidermal growth factor (EGF) was purchased from Toyobo (Osaka, Japan). PTV was purchased from Kowa Company, Ltd. (Tokyo, Japan). Anti-HCV core antibody (CP11) was purchased from the Institute of Immunology (Tokyo, Japan), and anti-HCV NS5A antibody was the generous gift of Dr. A. Takamizawa (Research Foundation for Microbial Diseases, Osaka University). Antibodies specific to ERK1/2 (p44/42 MAPK), MEK1/2, and phosphorylated (S217/221) MEK1/2 were purchased from Cell Signaling Technology (Beverly, MA), and anti-phosphorylated (T202/Y204) ERK1/2 antibody was obtained from BD Biosciences (San Jose, CA). Anti–β-actin antibody was purchased from Sigma Aldrich.

Cell Cultures. The cell lines OR6 and sO were cloned from ORN/C-5B/KE RNA and subgenomic replicon RNA (ON/3-5B)–replicating cells, respectively (Fig. 1). These cells were derived from the hepatoma cell line HuH-7, cultured in Dulbecco's modified Eagle's medium supplemented with 10% fetal bovine serum (FBS), peni-

cillin, streptomycin, and 300 μg/mL of G418 (Geneticin; Invitrogen, Carlsbad, CA), and passaged twice a week at a 5:1 split ratio. ORN/C-5B/KE and ON/3-5B were derived from HCV-O (strain O of genotype 1b).[10]

OR6 Reporter Assay. For the RL assay, 1.0-1.5 $\times$ 10^4 OR6 cells were plated onto 24-well plates in triplicate and precultured for 24 hours. The cells were pretreated with DMSO or a specific inhibitor for 1 hour and then were treated with each anti-HCV nutrient or compound in either the absence (DMSO) or presence of a specific inhibitor for 72 hours. After the treatment, the cells were harvested with Renilla lysis reagent (Promega, Madison, WI) and subjected to RL assay according to the manufacturer's protocol.

Western Blot Analysis. For analysis of the effect of a specific inhibitor on the anti-HCV activity, 6.0-6.5 $\times$ 10^4 OR6 cells were plated onto 6-well plates and precultured for 24 hours. The pretreatment with DMSO or a specific inhibitor for 1 hour and subsequent treatment for 72 hours was performed in the same manner as for the OR6 reporter assay. For analysis of the activities of each anti-HCV nutrient or reagent on the MEK–ERK1/2 signaling pathway, 1.0 $\times$ 10^5 OR6 or sO cells were plated onto 6-well plates and precultured in 10% FBS-containing medium for 24 hours. After the preculture, the culture medium was changed to FBS-free medium and the cells were cultured for 48 hours prior to treatment with each nutrient or reagent. When the effect of a specific inhibitor or VE on ERK1/2 phosphorylation was analyzed, the cells were pretreated with the specific inhibitor or VE for 1 hour prior to each treatment. Preparation of the cell lysates, sodium dodecyl sulfate–polyacrylamide gel electrophoresis, and immunoblotting were then performed as described.[26]

Measurement of ROS. OR6 cells in 24-well plates were left untreated or were treated with hydrogen peroxide (1 mM), LA (200 μM), and CsA (15 μg/mL) for 30 minutes and then incubated with dihydrodichlorocarboxyfluorescein diacetate (Invitrogen) (5 μM) for 15 minutes. Fluorescence was measured with a FLUOROSKAN ASCENT fluorescence plate reader (Thermo Fisher Scientific, Waltham, MA) at an excitation wavelength of 485 nm and emission wavelength of 535 nm.

Cell Growth Assay. To examine the activity of EGF on OR6 cell growth, 6.0-6.5 $\times$ 10^4 OR6 cells were plated onto 6-well plates in triplicate and were pre-cultured for 24 hours. The cells were treated with or without EGF for 72 hours, and the number of viable cells was counted after trypan blue dye treatment as described.[11]

Statistical Analysis. Statistical comparison of the luciferase activities between the various treatment groups was performed using the Student t test. P values of less than 0.05 were considered statistically significant.

Results

Effects of MEK1/2-Specific Inhibitors on the Anti-HCV Activities of BC, VD2, and LA in OR6 Cells. Our recent study suggested the involvement of oxidative stress in the suppressive mechanism of three anti-HCV nutrients: BC, VD2, and LA.[13] Because there have been reports of negative regulation of HCV RNA replication via the MEK–ERK1/2 signaling pathway,[24,25] which is one of the oxidative stress-induced cellular signaling pathways, we hypothesized that the suppression of HCV RNA replication by these three nutrients might be mediated via this cascade (Supporting Fig. 1). To test this hypothesis, we first used an OR6 assay system to examine the effects of U0126 and PD98059, inhibitors specific to MEK1/2, on the three anti-HCV nutrients at 60% inhibitory concentration. As shown in Fig. 2A, treatment with either 5 μM of U0126 or 10 μM of PD98059 slightly enhanced HCV RNA replication in comparison with the control. However, U0126 attenuated the anti-HCV activities of the three nutrients more clearly than PD98059 (Fig. 2A,B). U0126 prevented the anti-HCV activities of the three nutrients in a significant and dose-dependent manner and exerted complete inhibition against the anti-HCV activities of BC and LA (Fig. 2C,D), while the inhibitory effect of PD98059 was more mild (Fig. 2E,F). As shown in Fig. 2G, we also found that U0126 treatment restored the expressions of HCV proteins, core, and NS5A in a dose-dependent manner. We further demonstrated that knockdown of MEK1 or MEK2 by small interfering RNA negated the anti-HCV activity of LA (Supporting Fig. 2A-C). These inhibitions by U0126 against the anti-HCV activities of the three nutrients were not due to the enhancement of encephalomyocarditis virus/internal ribosomal entry site–driven RL activity, because this activity was not increased by U0126 (data not shown). Moreover, treatment with neither SB203580 (an inhibitor specific to p38 MAPK) nor c-Jun N-terminal kinase inhibitor, both of which belong to the same cascade family as MEK–ERK1/2, significantly affected the anti-HCV activities of the three nutrients (data not shown). These results imply that the activation of the MEK–ERK1/2 signaling pathway might be required for the suppression of genome-length HCV RNA replication by the three nutrients in cell culture.

Effect of U0126 on the Suppressive Effects of Polyunsaturated Fatty Acids and Anti-HCV Reagents in OR6 Cells. Previous studies using a cell culture system have shown that polyunsaturated fatty acids (PUFAs), including LA, act as anti-HCV nutrients.[27,28] A recent study reported that lipid peroxidation of PUFAs was correlated with their anti-HCV activities, which were pre-

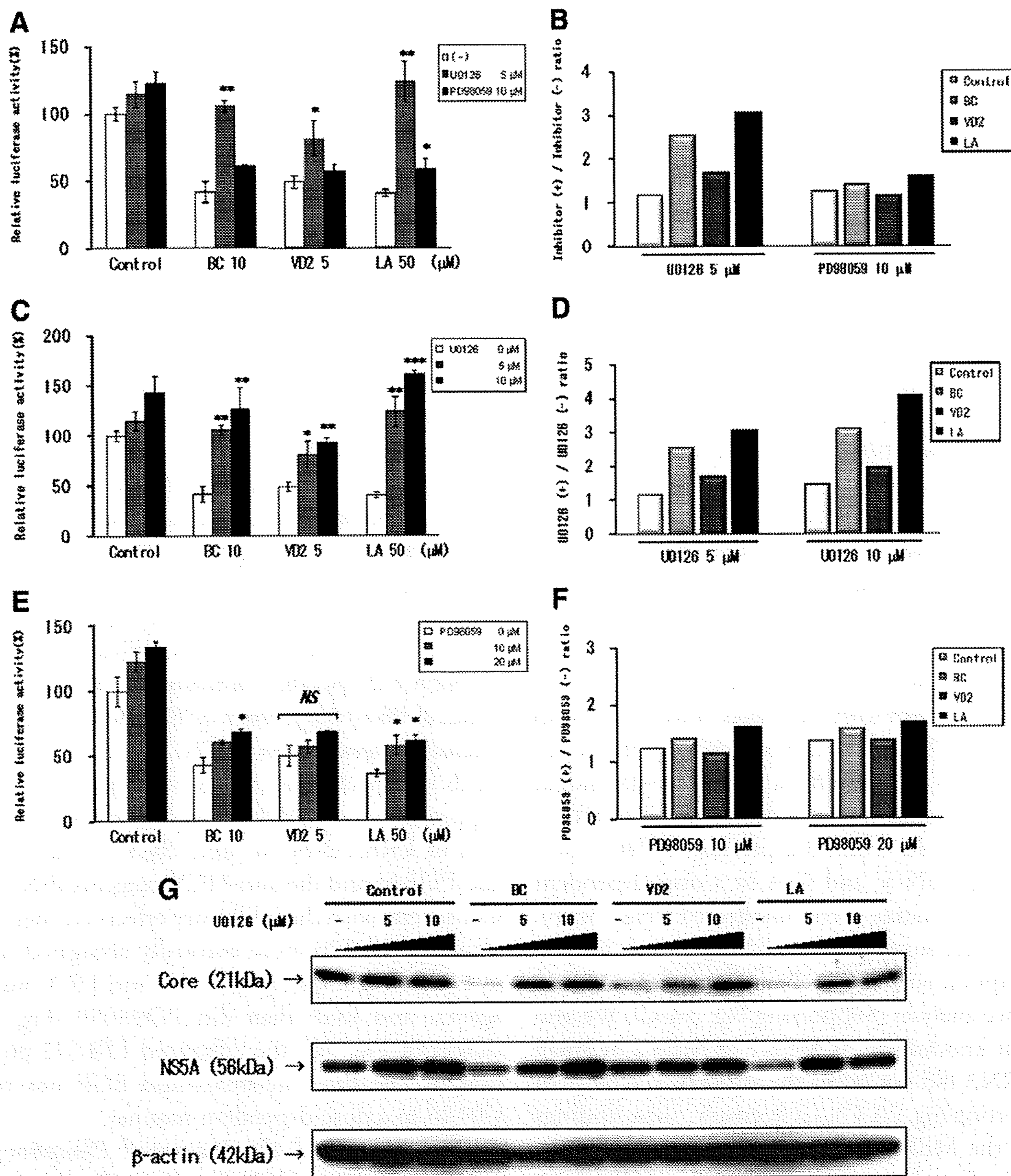

Fig. 2. U0126 strongly inhibited the anti-HCV activities of the anti-HCV nutrients BC, VD2, and LA in OR6 cells. (A,B) Effects of MEK-specific inhibitors on the three nutrients at the 60% inhibitory concentration. OR6 cells were pretreated with DMSO, 5 μM U0126, or 10 μM PD98059 for 1 hour. The cells were then treated with control medium, 10 μM BC, 5 μM VD2, or 50 μM LA in either the absence (DMSO) or presence of each specific inhibitor for 72 hours. After treatment, RL assay was performed as described in Materials and Methods. Shown here is the relative luciferase activity (%) calculated when the RL activity of the control was assigned as 100%. Data are expressed as the mean $\pm$ standard deviation of triplicate samples from at least three independent experiments. Asterisks indicate significant difference from treatment with DMSO (*$P < 0.05$; *$P < 0.01$) (A). The ratio of the RL activity in the presence of the MEK-specific inhibitor to the RL activity in the absence of the inhibitor was then calculated (B). (C-F) OR6 reporter assays of the dose effects of MEK1/2-specific inhibitors on the three nutrients. OR6 cells were pretreated with DMSO, U0126 (C), or PD98059 (E) at the indicated concentrations for 1 hour. Treatment of the cells with control medium or each of the three nutrients in either the absence (DMSO) or presence of each specific inhibitor and the RL assay of harvested OR6 cell samples were performed as described in panels A and B. Asterisks indicate significant difference from treatment with DMSO (*$P < 0.05$; **$P < 0.01$; ***$P < 0.001$; NS, not significant). Next, we calculated the ratio of RL activity in the presence of the MEK-specific inhibitor, U0126 (D), or PD98059 (F), to the RL activity in the absence of the inhibitor. (G) Western blot analysis of the dose effects of U0126 on three nutrients. OR6 cells were pretreated and then treated as in panel C. The production of HCV core and NS5A in the cells was analyzed by way of immunoblotting using antibodies specific to HCV core (top row) and NS5A (middle row). β-actin was used as a control for the amount of protein loaded per lane (bottom row).

vented by treatment with VE.[29] This result coincides with our previous observations on the effects of LA.[13] We proposed that the MEK–ERK1/2 signaling pathway might be involved in the anti-HCV activity of PUFAs, including LA, because lipid peroxidation is known to be a ROS-triggered cellular modification.[16] As expected, treatment with U0126 attenuated the anti-HCV activities of four representative PUFAs in a significant and dose-dependent manner (Fig. 3A,B).

Moreover, because the anti-HCV activities of BC, VD2, LA, and CsA, but not FLV, were found to be negated by VE,[13] we were also interested in the potent role of the MEK–ERK1/2 signaling pathway in the anti-HCV mechanism of CsA. Furthermore, the previous study using a subgenomic replicon system had already shown the partial involvement of this cascade in the antiviral activity of IFN-γ.[24] Therefore, we examined the effects of U0126 on various anti-HCV reagents: IFN-γ, CsA, and statins (FLV and PTV). We confirmed that also in genome-length HCV RNA replication cells, U0126 significantly inhibited the anti-HCV activity of IFN-γ (Fig. 3C,D). Interestingly, consistent with the effects of treatment with VE,[13] the anti-HCV activity of CsA was completely abrogated by U0126 in a significant and dose-dependent manner, whereas statins were unaffected (Fig. 3C,D).

U0126 restored the reduced expression of HCV proteins by PUFAs, IFN-γ, and CsA in a dose-dependent manner, whereas statins were unaffected (Fig. 3E,F). These results were supported by additional real-time reverse-transcription polymerase chain reaction and immunofluorescence analyses (Supporting Fig. 3A-C). We also observed that knockdown of MEK1 or MEK2 by small interfering RNA did not affect the anti-HCV activity of PTV (Supporting Fig. 2A-C). Collectively, these findings suggest that the MEK–ERK1/2 signaling pathway may play a critical role in the negative regulation of HCV RNA replication by the anti-HCV nutrients BC and VD2, PUFAs, and the anti-HCV reagents IFN-γ and CsA, but not statins.

Activation of the MEK–ERK1/2 Signaling Pathway by Anti-HCV Nutrients and Reagents. To further ensure the involvement of the MEK–ERK1/2 signaling pathway in the suppressive mechanisms of anti-HCV nutrients and reagents, we next examined whether these nutrients and reagents could actually initiate the activation of this signaling pathway. After treating the HCV RNA replicating cells with each of the nutrients and reagents, we performed immunoblotting specific to the phosphorylation of ERK1/2 and MEK1/2. In the same way as EGF, a potent activator of these kinases, the three anti-HCV nutrients (BC, VD2, and LA) enhanced the phosphorylation of ERK1/2 and MEK1/2 in both genome-length and subgenomic HCV RNA replication cells (Fig. 4A,B). IFN-γ, CsA, and all of the PUFAs also up-regulated this cascade in OR6 cells (Fig. 4C,D). The increase in phosphorylation of ERK1/2 was not observed after either statin treatment (Fig. 4D). The activation of MEK–ERK1/2 by the three anti-HCV nutrients was apparent until 1 hour after their application and subsequently attenuated, although EGF exhibited persistent enhancement of MEK–ERK1/2 phosphorylation (Fig. 4E). Because the experiments regarding ERK1/2 phosphorylation were performed in FBS-free conditions, we checked the anti-HCV activity of PTV, CsA, and LA in FBS-free medium. The results revealed that these anti-HCV reagents and nutrients also inhibited HCV RNA replication in FBS-free conditions (Supporting Fig. 4). Taken together, these findings indicate that the anti-HCV nutrients and reagents activated the MEK–ERK1/2 signaling pathway in HCV RNA replicating cells, providing further confirmation that this signaling cascade might be involved in their anti-HCV activities.

MEK1/2-Specific Inhibitors Attenuated the Increased Phosphorylation of ERK1/2 by Anti-HCV Nutrients/Reagents and EGF. We next tested whether MEK1/2-specific inhibitors could prevent not only the suppression of HCV RNA replication but also the activation of ERK1/2 by the anti-HCV nutrients BC, VD2, and PUFAs and the anti-HCV reagents IFN-γ and CsA. Consistent with the inhibitory effects on their anti-HCV activities, U0126 more markedly abrogated the increase in ERK1/2 phosphorylation by anti-HCV nutrients, reagents, and EGF than did PD98059 (Fig. 5A,B). As shown in Fig. 5C, the enhanced ERK1/2 phosphorylation by the three nutrients and EGF was reduced by U0126 in a dose-dependent manner.

VE Attenuated the Increased Phosphorylation of ERK1/2 by Anti-HCV Nutrients/Reagents and EGF. Because the suppression of HCV RNA replication by BC, VD2, LA, and CsA were completely negated by the treatment with VE in our recent study,[13] we investigated whether VE could also inhibit ERK1/2 activation by anti-HCV nutrients and reagents. As expected, VE also attenuated the enhanced phosphorylation of ERK1/2 by not only anti-HCV nutrients and CsA but also IFN-γ and EGF (Fig. 6A,B). We also demonstrated that phosphorylation of ERK1/2 by CsA was attenuated with *N*-acetylcysteine treatment and led to the negation of inhibition of HCV RNA replication (Supporting Fig. 5A-C). The anti-HCV nutrients and reagents, whose activities were negated by U0126, were also inhibited by VE. In contrast, the anti-HCV activities of statins were not negated by U0126 or VE. We also demonstrated that LA and CsA induce ROS (Fig.

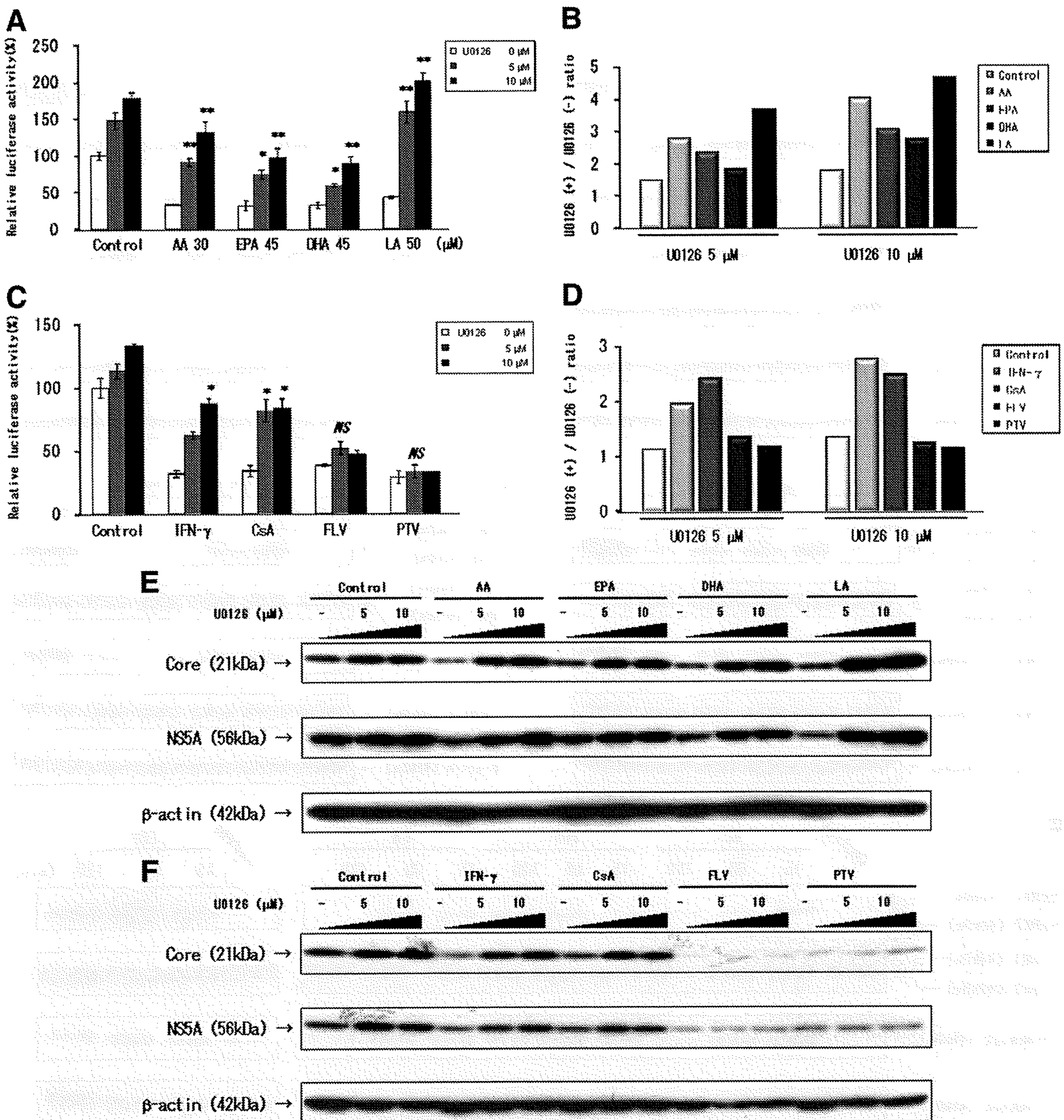

Fig. 3. U0126 dose-dependently attenuated the anti-HCV activities of PUFAs, IFN-γ, and CsA, but not the statins. (A-D) OR6 reporter assays of the dose effects of U0126 on the PUFAs and anti-HCV reagents at the 60% inhibitory concentration. OR6 cells were pretreated with DMSO or U0126 as in Fig. 2C and then treated with control medium, 30 μM AA, 45 μM EPA, 45 μM DHA, or 50 μM LA (A) and control medium, 0.4 IU/mL IFN-γ, 0.2 μg/mL CsA, 3 μM FLV, or 1 μM PTV (C), respectively, in either the absence (DMSO) or presence of U0126 for 72 hours. After the treatment, the RL assay of harvested OR6 cell samples was performed as described in Fig. 2A and 2B. Asterisks indicate significant difference from treatment with DMSO (*$P < 0.05$; **$P < 0.01$; NS, not significant). The ratio of the RL activity in the presence of U0126 to the RL activity in the absence of U0126 was then calculated (B, D). (E, F) Western blot analysis of the dose effects of U0126 on the PUFAs and anti-HCV reagents. The production of HCV core (top row) and NS5A (middle row) in the cells treated as in panel A (E) and panel C (F) was analyzed as described in Fig. 2G. β-actin was used as a control for the amount of protein loaded per lane (bottom row).